

# Microscopic and macroscopic properties of carbohydrate solutions in the ionic liquid 1-ethyl-3- methyl-imidazolium acetate

Michael E. Ries <sup>a,\*</sup>, Asanah Radhi <sup>a</sup>, Stephen M Green <sup>a</sup>, Jamie Moffat <sup>b</sup> and Tatiana Budtova <sup>c</sup>

<sup>a</sup> Soft Matter Physics Research Group, School of Physics and Astronomy, University of Leeds,  
Leeds, LS2 9JT. UK.

<sup>b</sup> Innovia Films R&D Centre, West Road, Wigton, Cumbria CA7 9XX, United Kingdom

<sup>c</sup> MINES ParisTech, PSL Research University, Center for Materials Forming (CEMEF), UMR  
CNRS 7635, CS 10207, 06904 Sophia Antipolis, France.

[m.e.ries@leeds.ac.uk](mailto:m.e.ries@leeds.ac.uk)

**Keywords:** cellulose, cellobiose, glucose, carbohydrate, ionic liquid, NMR, relaxometry, viscosity, diffusion.

## ABSTRACT

Solutions of glucose, cellobiose and microcrystalline cellulose in the ionic liquid 1-ethyl-3-methylimidazolium acetate ([C2mim][OAc]) have been examined using low field (20 MHz) NMR relaxometry and rheology. The spin-lattice ( $T_1$ ) and spin-spin ( $T_2$ ) relaxation times have been determined from 30 °C to 70 °C inclusive, for a range of concentrations (0 to 15 wt %) of each carbohydrate in [C2mim][OAc]. The zero shear rate viscosities for the same samples across the same temperature range were studied. The viscosity, NMR relaxometry and previously published diffusion data were all analysed together through the Debye-Stokes-Einstein equations. Microscopically these systems behave as an “ideal mixture” of free ions and ions associated with the carbohydrate molecules. The molar ratio of carbohydrate OH groups to ionic liquid molecules,  $\alpha$ , is the key parameter in determining the NMR relaxometry and hence the local microscopic environment of the ions. NMR relaxometry data are found to follow an Arrhenius type behavior and the difference in rotational activation energy between free and associated ions is determined at  $6.2 \pm 0.5$  kJ/mol.

## 1. INTRODUCTION

In 1914 Walden defined an ionic liquid (IL) to be a salt, which has a liquid state below 100 °C at atmospheric pressure.<sup>1</sup> Since then, and particularly more recently, there has been much research into using ILs as “green” solvents.<sup>2-7</sup> This is because their properties can include low to negligible vapor pressure, high thermal stability, low flammability and the ability to dissolve natural compounds such as polysaccharides.<sup>8</sup> In 1934, Graenacher<sup>9</sup> obtained a patent for, amongst other things, dissolving cellulose with molten *N*-ethylpyridinium chloride. This salt has a melting point at 118 °C and therefore does not fall under the prior Walden definition of an ionic liquid. Swatloski et al in 2002 published on the use of imidazolium based ionic liquids to dissolve cellulose.<sup>10</sup> In this work the authors measured the solubility of cellulose in a variety of salts and found that 1-butyl-3-methyl-imidazolium chloride [C4mim][Cl] dissolved the greatest amount of cellulose, up to 25 wt % upon microwave heating.

It is often said that cellulose is the world’s most abundant biopolymer, and it is indeed one of the most studied with the term “cellulose” dating back to 1839 and the pioneering work of Payen.<sup>11</sup> As cellulose does not melt, the processing of cellulose requires dissolution and/or derivatisation, with objects such as fibres and films being formed. Therefore, understanding cellulose dissolution is a very important topic. Despite this and the long history of cellulose research, the dissolution of cellulose is still puzzling and consequently generates much research output.<sup>12</sup> Commonly in the literature<sup>13</sup> the reason given for the insolubility of cellulose in water and typical organic solvents is the many intra- and inter-hydrogen bonds present.<sup>14</sup> Recently though the “Lindman hypothesis” reminded the community that cellulose is amphiphilic and that the hydrophobic interactions will also be an important aspect of the solubility of cellulose.<sup>15</sup>

Understanding the dissolution of cellulose is an active topic, involving various experimental tools and molecular modelling.<sup>13, 16-38</sup> For example, Gentile and Olsson<sup>17</sup> used pulsed field gradient (PFG) nuclear magnetic resonance (NMR) to measure the self-diffusion coefficients in solutions of microcrystalline cellulose and dissolving pulp in aqueous tetrabutylammonium hydroxide (TBAH). It was demonstrated that the TBA<sup>+</sup>hydrogen ions and the water molecules had a distinct diffusion dependence on cellulose concentration, indicating quite different molecular interactions with cellulose. One key result was that TBAH binds to cellulose such that there are 1.2 ions associated with each glucose unit, with this number being independent of the cellulose molecular weight. An extensive study was carried out by Zhang et al<sup>32</sup> in which the solubility of carbohydrates was examined across ionic liquids consisting of eleven different cations and four different anions. The authors used <sup>1</sup>H and <sup>13</sup>C NMR spectroscopy and tracked the change in chemical shift of the various resonances as a function of cellobiose concentration. It was shown that the hydrogen bond interaction between the ions and the hydroxyl groups (OH) on the cellobiose is the dominant process in the dissolution. The anions associated with the hydrogen atoms of the OH groups, whereas the cations associated with the oxygen atoms. Computer simulation work by Bharadwaj et al<sup>16</sup> examined glucose and cellobiose in water and three imidazolium based ionic liquids. It was found that increasing the alkyl chain length of the cation did not alter the solvation of the OH groups of the cellobiose and glucose by the acetate anion. Fourier transform infrared spectroscopy (FTIR) and multi nuclear NMR spectroscopy were combined with conductivity measurements by Zhang et al<sup>30</sup> to determine the molecular interactions in solutions of cellulose and *N,N*-dimethylacetamide (DMAc)/LiCl. They showed that Li<sup>+</sup> - Cl<sup>-</sup> pairs are broken and the Cl<sup>-</sup> then forms strong hydrogen bonds with the OH groups of cellulose. Fully atomistic molecular dynamic simulations by Schutt et al<sup>28</sup> examined the effect of

adding oxygen atoms to the tail of an imidazolium cation on cellulose dissolution, using cellobiose and glucose as model cellulose compounds. The modification of the solvent tail was found to lower its viscosity, with the anion's interactions with the OH groups of the glucose or cellobiose playing a key role in determining the bulk solution properties. Zhao et al<sup>39</sup> used molecular dynamic simulations and quantum chemistry calculations to examine the effects of co-solvent on cellulose dissolution in imidazolium based ionic liquids; they showed that the dissolution of cellulose is mainly determined by hydrogen bond interactions between the anion and hydroxyl protons of cellulose. From this very brief overview of articles concerning the solubility of cellulose it is clear that the solvent – cellulose OH group interactions play a major part in understanding the dissolution of cellulose.

In this work we will examine solutions of cellulose, cellobiose and glucose in the ionic liquid 1-ethyl-3-methyl-imidazolium acetate ([C2mim][OAc]), currently<sup>16</sup> one of the most commonly used ILs in cellulose dissolution. Here we will demonstrate the importance of the molar ratio of carbohydrate hydroxyl groups to ions, showing that this is a key parameter in determining the microscopic dynamics within these systems. The zero shear rate viscosity and low field (20 MHz) NMR relaxometry will be analyzed and then combined through the Stokes-Debye-Einstein relationship. This will enable us to compare and contrast the macroscopic and microscopic properties, showing key differences between the cellulose, cellobiose and glucose solutions. The NMR relaxometry data will be analyzed using Bloembergen-Purcell-Pound (BPP) theory<sup>40</sup> and it will be argued that the correlation times obtained from this approach correspond to the rotational correlation times of the ions within the solutions. Finally, previous published data<sup>37</sup> for the ions' self-diffusion coefficients in the very same solutions will be combined with the relaxometry analysis and viscosity results, in order to explain the difference in activation energy for diffusional

and rotational processes. This analysis will also give information on the additional activation energy for ions to bind to each carbohydrate.

## 2. EXPERIMENTAL

### 2.1. Materials and sample preparation

Glucose, cellobiose and cellulose (Avicel PH-101, with a degree of polymerization of 180 as given by the manufacturer) were purchased from Sigma Aldrich and prior to dissolution these materials were dried under vacuum at 70 °C for a minimum period of 12 hours. The structures of glucose, cellobiose and cellulose<sup>14</sup> are shown below, in Figure 1. The ionic liquid 1-ethyl-3-methyl-imidazolium [C2mim][OAc] (97% purity) was purchased from Sigma Aldrich and used without any further purification. Neat [C2mim][OAc] and three sets of samples (glucose / cellobiose / cellulose) each with five concentrations of the corresponding carbohydrate (1, 3, 5, 10, and 15 wt %) in [C2mim][OAc] were prepared. Diffusion data from our previous publication<sup>37</sup> on the same systems is also included in this work.

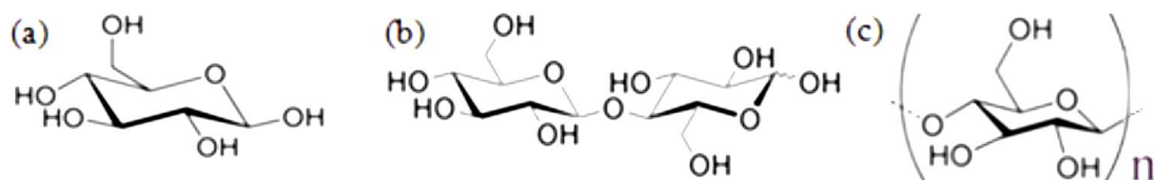


**Figure 1.** Structure of a) glucose b) cellobiose and c) cellulose.

The sample preparations were made in an MBraun Labmaster 130 atmospheric chamber under nitrogen, providing a dry environment, with the chamber being maintained at a dew point level between -70 and -40 °C, corresponding to less than 0.5 ppm of water. The [C2mim][OAc] and

glucose / cellobiose / cellulose were combined and stirred in a container at 50 °C for a minimum of 48 hours. A small quantity of each carbohydrate [C2mim][OAc] solution was then placed in a standard 5 mm NMR tube within the chamber. Each tube was sealed still within the chamber to prevent moisture contamination and when the samples were not in use they were stored in a desiccator. Karl-Fischer titration indicated that all the samples had less than 0.3 wt % water. From our previous work<sup>33</sup> we found that for water concentrations of 0.5 wt % and above, a clearly visible water resonance appears in the high field (Bruker Biospin 400 MHz) spectra. All our samples were checked by high resolution <sup>1</sup>H NMR in a Bruker Avance II 400 MHz spectrometer for impurities and no degradation or decomposition was observed.<sup>41</sup>

## **2.2. Low Field NMR Relaxometry**

The spin–lattice relaxation time  $T_1$  and spin–spin relaxation time  $T_2$  were determined for each of our samples in steps of 10 °C between 30 and 70 °C inclusive, using a 20 MHz Maran Benchtop NMR spectrometer. Temperature control was within +/- 0.1 °C. The inversion recovery method was used to measure  $T_1$  and the Carr–Purcell–Meiboom–Gill (CPMG) pulse sequence for  $T_2$ .<sup>42</sup> At each temperature, the samples were left to equilibrate for 10 min before measurements were recorded. The 90° pulse width was 3.7 μs, the signal was averaged across 8 scans, and the repetition time was set to at least  $5 \times T_1$ . In the inversion recovery experiment a linear increment time step of  $\sim \frac{1}{2} T_1$  was used with 15 increment steps being recorded. For the CPMG sequence 2000 echoes were used to give a total relaxation time of  $\sim 5 T_2$ . Single exponential fits were found to model the NMR relaxation curves very closely for all our results. We estimate the uncertainty on our NMR relaxation times to be less than 5%.

### 2.3. Viscosity

A Bohlin Gemini Advanced Rheometer equipped with 4°-40 mm cone plate was used to measure the viscosity of the solutions as a function of shear rate. The temperature range was from 10-100 °C in 10 °C increments. A thin film of low viscosity silicon oil was placed around the borders of the measuring cell in order to prevent moisture uptake.

## 3. RESULTS AND DISCUSSION

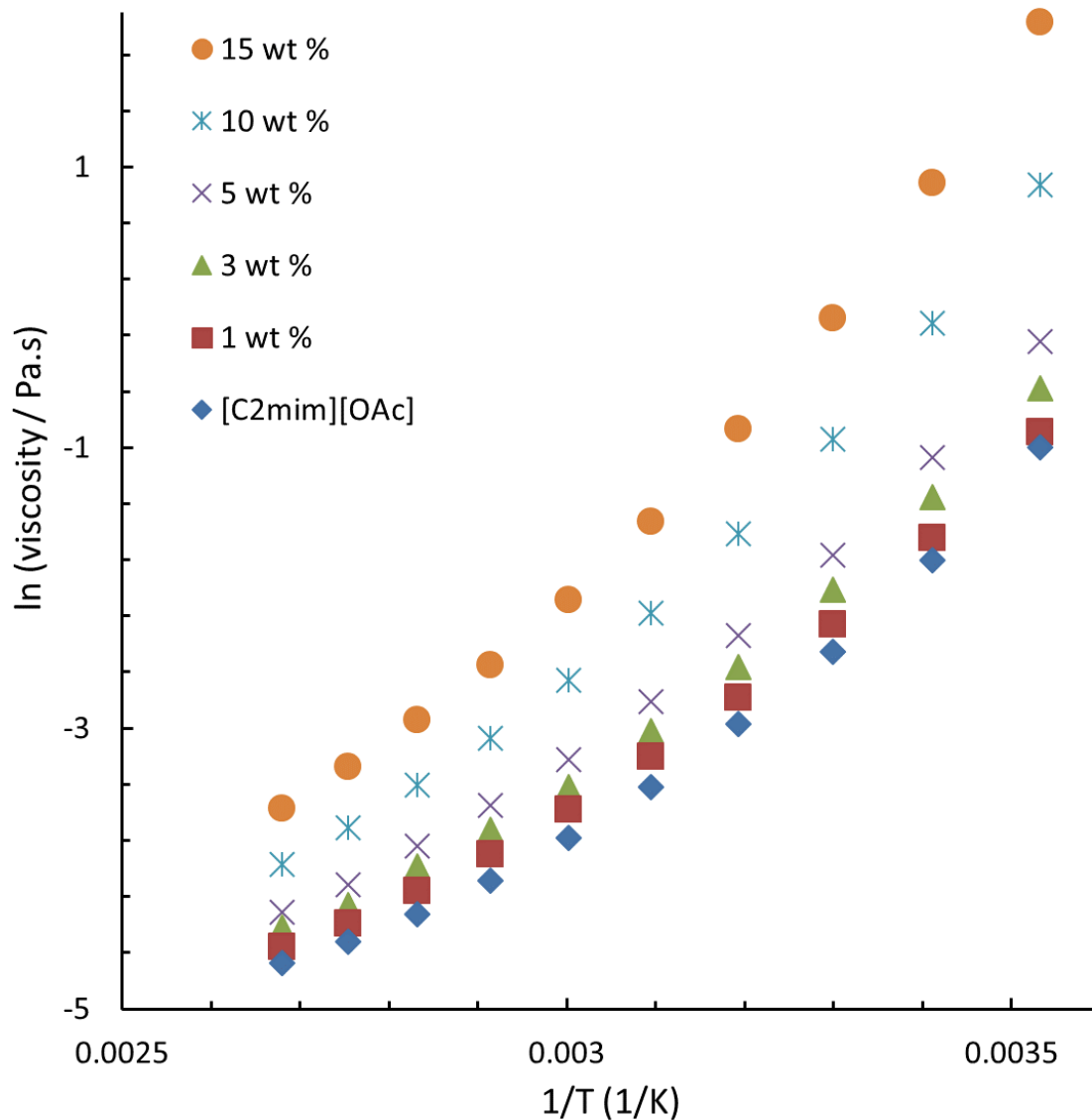
### 3.1. Viscosity

In the Supplementary Information, Figure SI1 shows the viscosity as a function of shear rate for a selection of glucose and cellobiose-[C2mim][OAc] solutions at 30 °C, demonstrating a Newtonian flow over a wide range of shear rates. This plateau value was then used as the zero shear rate viscosity, simply “viscosity”, in all later analyses. Figure SI2 shows that for any given concentration and temperature, cellobiose solution viscosity is very close to that of glucose, well within a 5% difference. This result was expected as far as both glucose and cellobiose are low molecular weight compounds and the volumes occupied by each molecule is comparable, at least on the length scales probed by viscosity. We have previously published<sup>13</sup> the viscosity values for solutions of cellulose-[C2mim][OAc]. Unsurprisingly, due to the polymeric nature of cellulose, its solution viscosity is between one and three orders of magnitudes higher than those of the glucose results presented here, see Figures SI3 and SI4 in the Supplementary Information.

The temperature dependence of the viscosity for the glucose samples is shown in Figure 2, indicating a non-Arrhenius behavior in the large temperature range studied here. Similar non-linear dependence has already been reported for cellulose-[C2mim][OAc] and cellulose-[C4mim][Cl] solutions, and it was demonstrated that this is induced by the behaviour of the ionic liquid itself.<sup>13</sup>



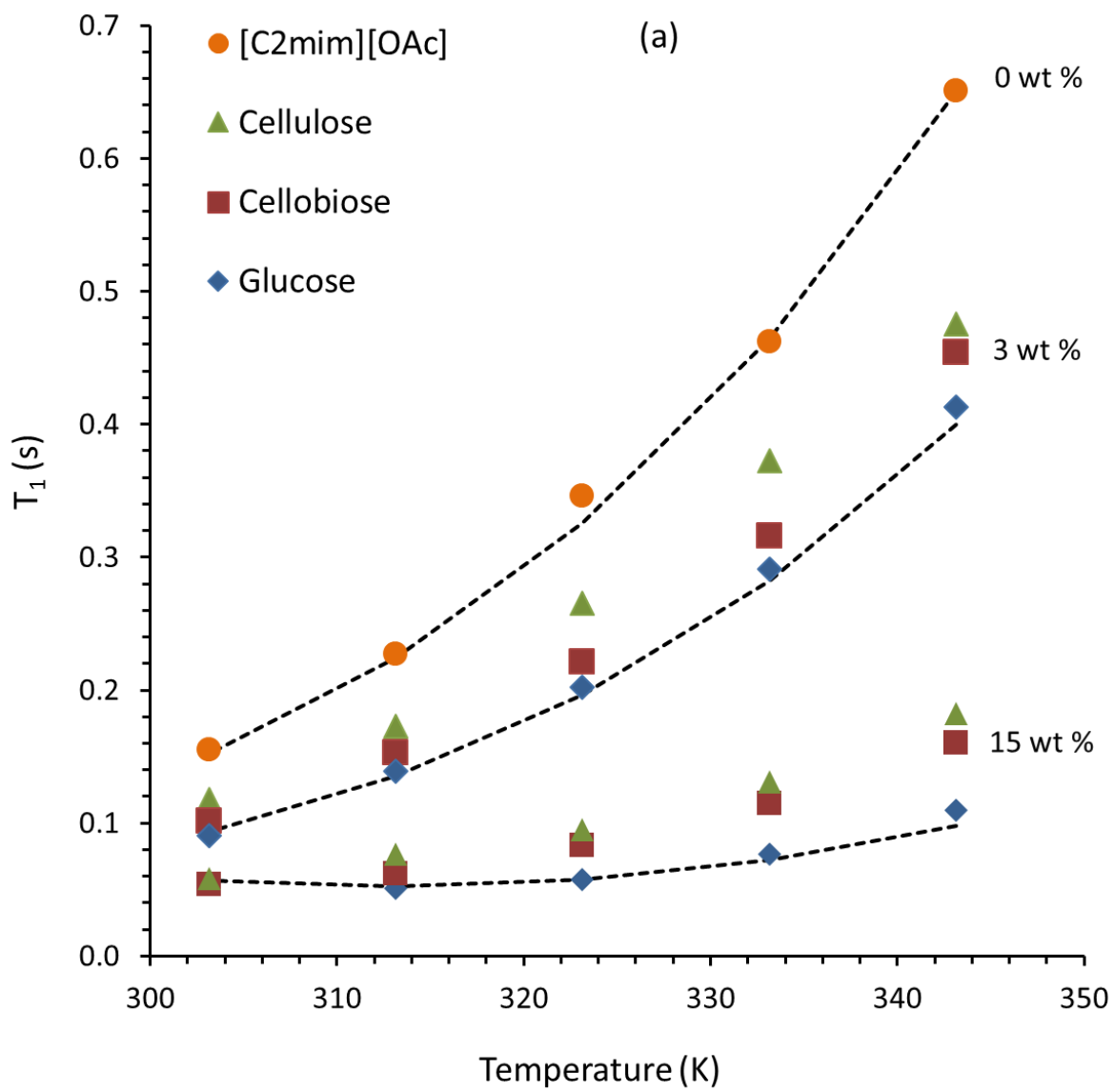
For further discussions on “fragile” behaviour in liquids, including ionic liquids, the reader is pointed to the seminal work<sup>43</sup> by Angell.



**Figure 2.** Viscosity of glucose-[C2mim][OAc] solutions as a function of inverse temperature at different concentrations of glucose. Error bars are within the size of the symbols shown.

### 3.2. NMR relaxation of ions in glucose, cellobiose and cellulose solutions

In Figure 3a the spin-lattice relaxation times  $T_1$  are shown for the pure ionic liquid [C2mim][OAc], 3 wt % and 15 wt % carbohydrate weight concentrations. Figure 3b shows the spin-spin relaxation times  $T_2$  for the same samples. As the majority of protons in these samples belong to the ionic liquid, even at the highest carbohydrate concentrations, it will be assumed that the NMR relaxometry is giving information predominantly about the motion of the ions in these solutions. In the 15 wt % samples 88% of the protons belong to the ionic liquid molecules. Furthermore, as this is a low field experiment (20 MHz), there is not sufficient chemical resolution to distinguish between cation and anion and so the relaxation times are in effect an average across both ions. The various dynamics or mechanisms that contribute to the NMR relaxation will be discussed in more detail later on.



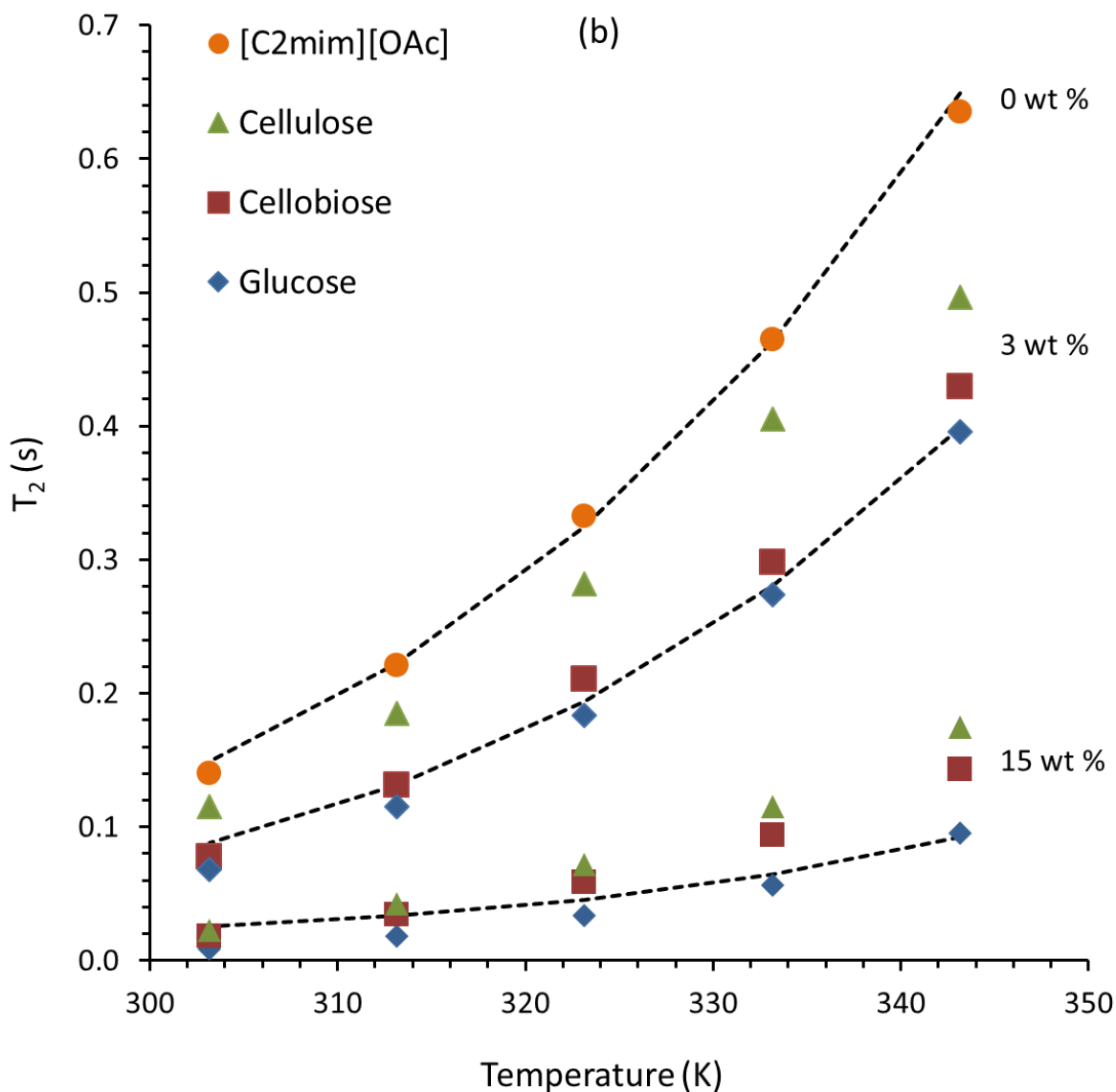


**Figure 3.** NMR relaxation times a)  $T_1$  and b)  $T_2$  of [C2mim][OAc] in glucose, cellobiose and cellulose solutions as a function of temperature, shown for three weight fractions 0 wt % (pure [C2mim][OAc]), 3 wt % and 15 wt %. Uncertainties are within the size of the symbols used. The dashed lines are fits of equation (2) to the 0 wt %, 3 wt % and 15 wt % glucose data.

Most of our data has  $T_1$  approximately equal to  $T_2$ , indicating that the results are within the “liquid”<sup>44</sup> like NMR response for the majority of our results; only at the highest carbohydrate

concentration of 15 wt % and at the lowest temperature 30 °C is  $T_1$  significantly larger than  $T_2$ . This means that with increase in temperature, and corresponding increase in the mobility of the ions, the relaxation times increase. On the other hand, as an increase in carbohydrate concentration is seen to decrease the NMR relaxation times this indicates a corresponding decrease in the mobility of the ions. The interactions between the ions and the carbohydrates are therefore reducing the mobility of the ions. It is interesting to note that, weight for weight, at any given temperature, the glucose NMR relaxation times are shorter than the cellobiose times, which again are shorter than the cellulose times. As these NMR relaxation times are related to the mobility of the ions this result is somewhat surprising, as this goes against what would have been expected from the viscosity results. The cellulose samples have the highest viscosity, but according to the NMR relaxometry data, the ions in the cellulose solutions have the highest mobility. Additionally, even though the glucose and cellobiose samples have the same viscosity, weight for weight, they are distinguishable in the NMR experiment, with their NMR relaxation times indicating that the mobility of the ions in these systems is significantly different. These results therefore strongly suggest that the local level or “micro” viscosity experienced by the ions is not simply related to the macroscopically determined zero shear rate viscosity.

In a recent publication<sup>37</sup> we measured the self-diffusion coefficients of ions in the very same systems on which we report here. In that previous work, it was found that glucose was the most effective at slowing down the diffusion of the ions and cellulose the least effective, with this perfectly reflecting the change in mobility indicated by the results obtained here on low field NMR relaxometry. The dependence of  $T_1$  on concentration of solute is displayed in Figure 4, showing glucose to be the most effective and cellulose the least effective at reducing  $T_1$ . Similar results are

found for the spin-spin relaxation times and can be found in the supporting information, see Figure SI5.

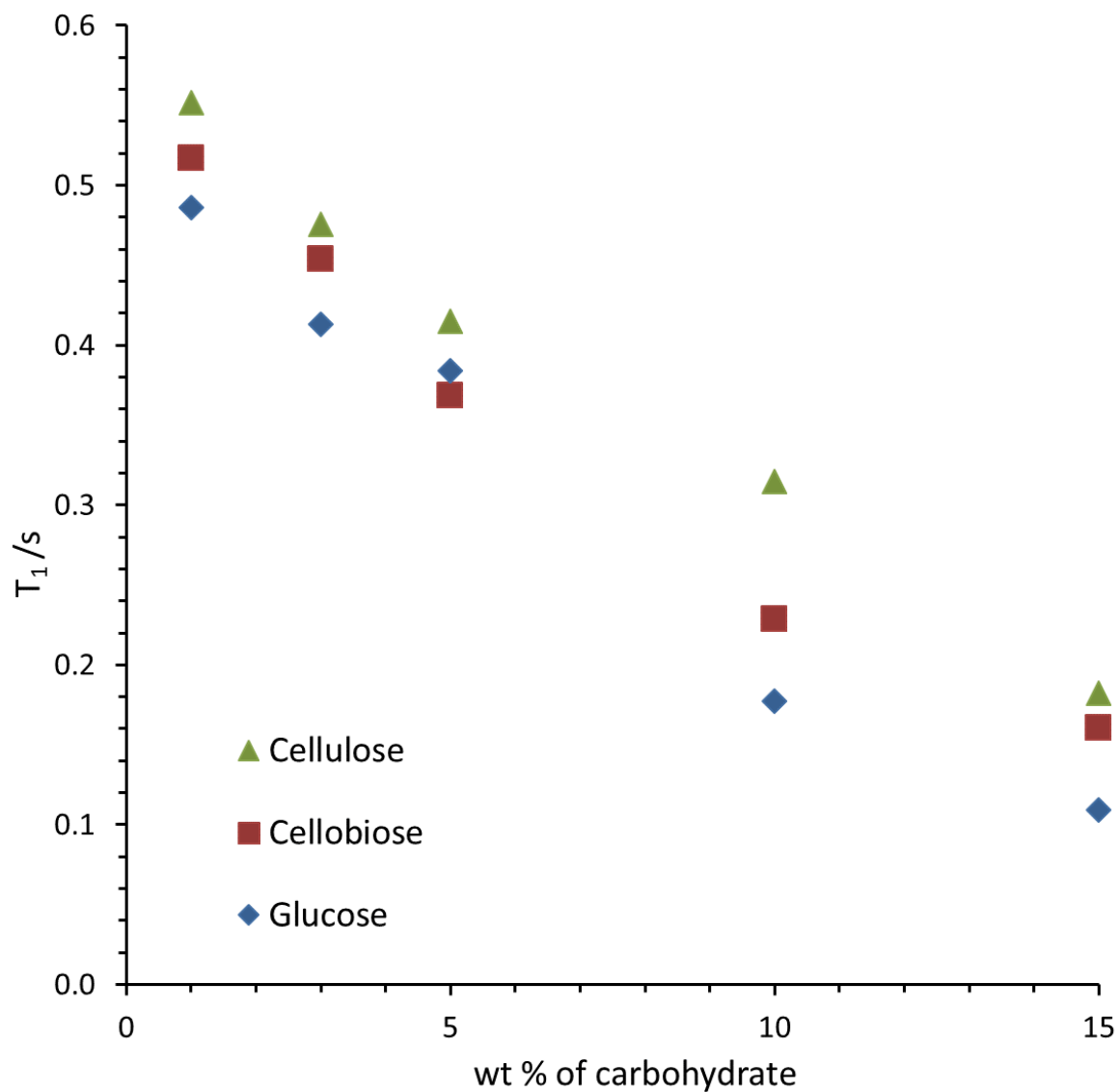
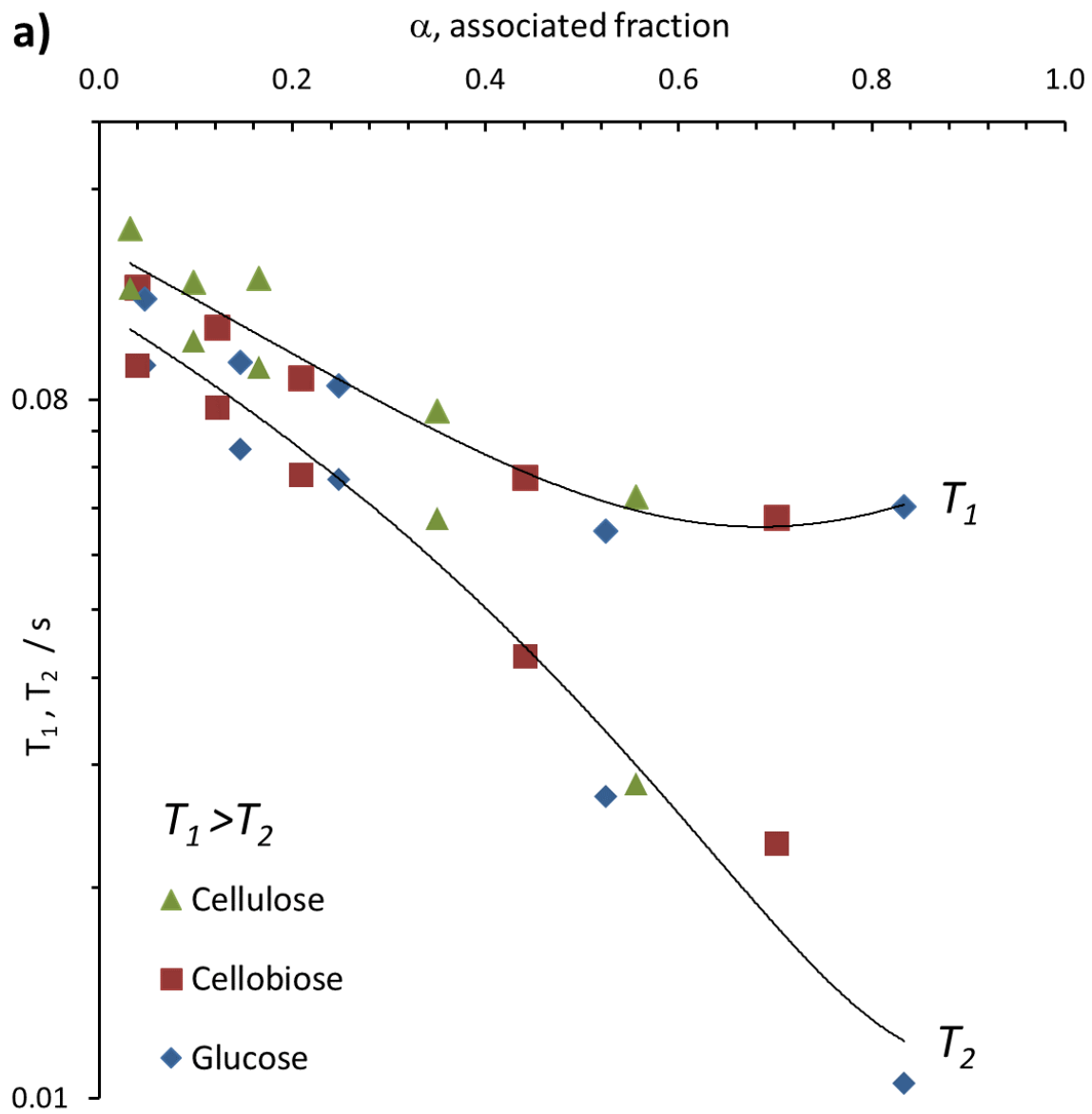


**Figure 4.** NMR spin-lattice relaxation times  $T_1$  for glucose, cellobiose and cellulose as a function of the wt % of carbohydrate in [C2mim][OAc] solutions, at 70 °C. Uncertainties are within the size of the symbols used.

In our recent article on diffusion<sup>37</sup> we introduced a parameter  $\alpha$ , termed the “associated fraction” of ions bound to the carbohydrate. Cellulose consists of D-anhydroglucopyranose units (AGU) joined together by  $\beta(1\rightarrow4)$  glycosidic bonds, each AGU unit within cellulose has three OH groups (Figure 1). Cellobiose is a disaccharide consisting of two *D*-Glucopyranoses linked by a  $\beta(1\rightarrow4)$  bond, each *D*-Glucopyranose in cellobiose has four OH groups. Finally, glucose is a monosaccharide with five OH groups. The term  $\alpha$  corresponds to a molar weight fraction, weighted to the number of OH groups from the “glucose units” (D-anhydroglucopyranose/Dglucopyranose/D-glucose unit) per [C2mim][OAc] molecule, and is given by<sup>37</sup>

$$\alpha = N \times \frac{M_{IL}}{M_{GU}} \times \frac{\phi}{100 - \phi} \quad (1)$$

where  $N$  is the number of OH groups per “glucose unit” (5, 4, 3 respectively for glucose, cellobiose and cellulose),  $M_{IL}$  is the molar mass of the ionic liquid (170 g/mol),  $M_{GU}$  is the molar mass of a “glucose unit” (180 g/mol, 171 g/mol, 162 g/mol respectively for glucose, cellobiose and cellulose) and  $\phi$  the weight percent of the carbohydrate in solution. We argued<sup>37</sup> that the molar ratio  $\alpha$  is the fraction of IL molecules involved in dissolving “glucose units” and therefore can be considered as an associated fraction of the ionic liquid. When the diffusion data was plotted as a function of  $\alpha$ , instead of carbohydrate weight fraction, then all the data from the different systems (glucose / cellobiose / cellulose) fell onto one master curve. In Figure 5 both  $T_1$  and  $T_2$  are plotted against  $\alpha$  for two temperatures, 30 °C and 70 °C, showing that master curves are obtained for the NMR relaxation times, as with the published<sup>37</sup> diffusion data, and this works both in the limit that  $T_1=T_2$  (*liquid* like regime) and when  $T_1>T_2$  (*solid* like regime).





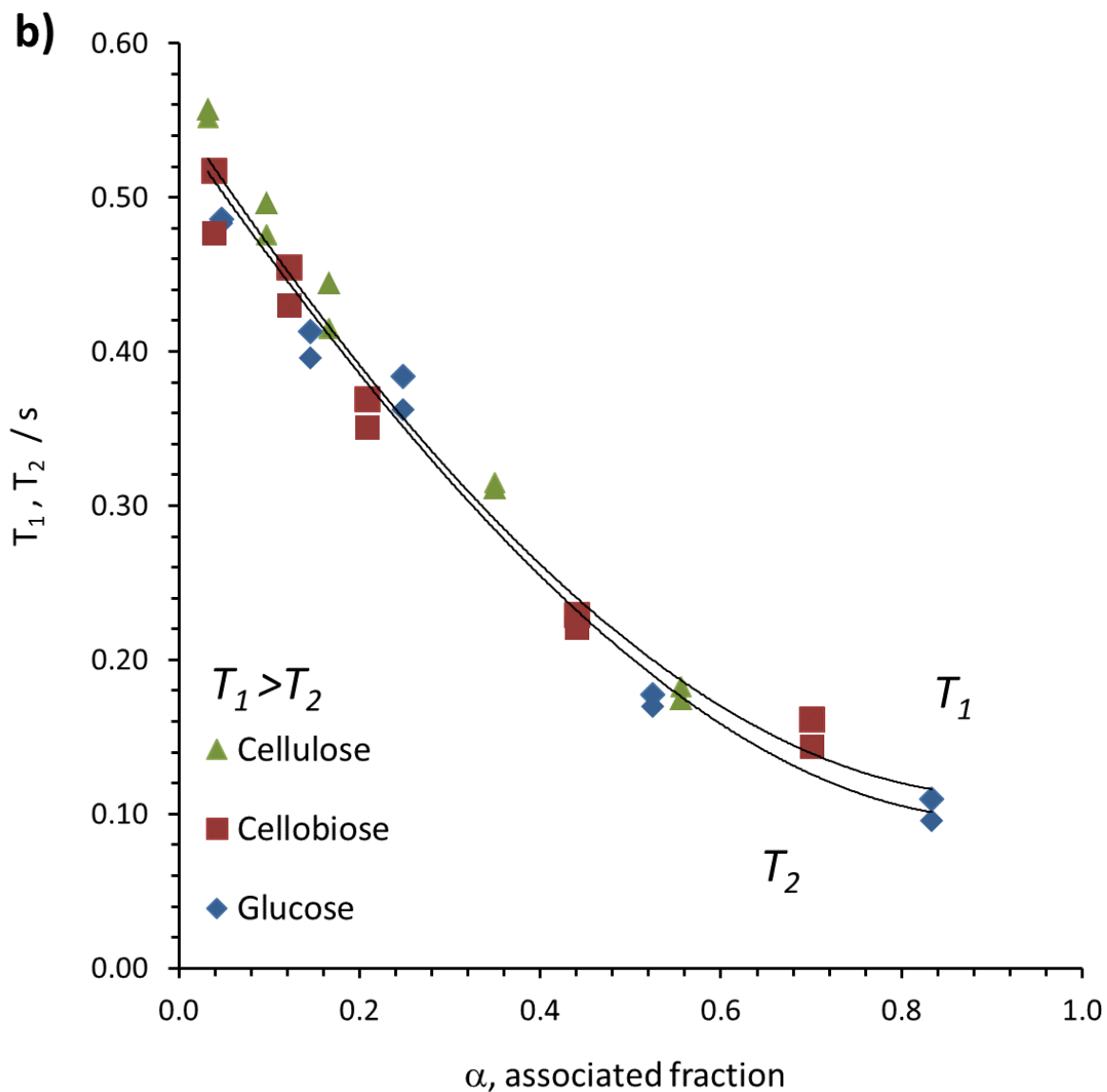


**Figure 5.** NMR spin-lattice relaxation times  $T_1$  and  $T_2$  for [C2mim][OAc] solutions with glucose, cellobiose and cellulose as a function of  $\alpha$  the associated fraction defined by equation (1) at **a) 30 °C** and **b) 70 °C**. Uncertainties are within the size of the symbols used. For all samples and all temperatures  $T_2 < T_1$ . Solid lines are given to guide the eye.

NMR relaxation times depend on the dynamics within the system being measured. Rotational and translational motions cause the magnetic fields at the protons to fluctuate. The benchtop analyzer used here operates at a Larmor frequency of 20 MHz, making both the  $T_1$  and  $T_2$  sensitive to molecular motion and consequent fluctuations at and around this frequency. For ionic liquids this corresponds to predominantly rotational motion;<sup>45</sup> for Larmor frequencies above 10 MHz the contribution to the NMR relaxation mechanisms from translational motion becomes less significant as the Larmor frequency is further increased.<sup>45-49</sup> In this article we will therefore make the working assumption that rotational motion of the ions is the dominant mechanism for the NMR relaxation and assume a single rotational correlation time  $\tau_R$  is responsible for determining both  $T_1$  and  $T_2$  for any given temperature and sample. This assumption can later be assessed by judging how successful it was in: i) modelling both spin-lattice and spin-spin relaxation times simultaneously across all samples and temperatures measured; ii) following quantitatively the Stokes-Debye-Einstein relationships; and iii) explaining the difference in activation energies from this analysis and those determined in our prior publication on the ions' self-diffusion coefficients.

According to Bloembergen, Purcell and Pound approach the NMR relaxation times can be related to a fluctuation correlation time, here assumed to be a rotational correlation time  $\tau_R$  for two protons at fixed distance  $r$  apart, as<sup>40, 50</sup>

$$\frac{1}{T_1} = K \left[ \frac{\tau_R}{1 + \omega_0^2 \tau_R^2} + \frac{4\tau_R}{1 + 4\omega_0^2 \tau_R^2} \right] \quad (2a)$$

$$\frac{1}{T_2} = \frac{K}{2} \left[ 3\tau_R + \frac{5\tau_R}{1 + \omega_0^2 \tau_R^2} + \frac{2\tau_R}{1 + 4\omega_0^2 \tau_R^2} \right] \quad (2b)$$

$$K = \frac{3}{10} \gamma^4 \hbar^2 \left( \frac{\mu_0}{4\pi} \right)^2 \frac{1}{r^6} \quad (2c)$$

where  $\omega_0$  is the Larmor frequency,  $\gamma$  the gyromagnetic ratio for protons,  $\hbar$  the reduced Planck constant,  $\mu_0$  the permeability of free space and  $r$  a system average or effective distance between protons. For each sample it will be assumed that there is an activation energy  $E_R$  for the rotation correlation time given by

$$\tau_R = \tau_0 \exp\left(\frac{E_R}{RT}\right) \quad (3)$$

where  $\tau_0$  is a constant sometimes referred to as the *high temperature* or *zero activation energy* rotational correlation time,  $R$  the gas constant and  $T$  the temperature in kelvin. When fitting the data,  $\tau_0$  and  $K$  will be taken as a global fitting parameters as they are related to the moment of inertia of the ions and the distance between protons respectively,<sup>51</sup> which should not change significantly with solute type (glucose / cellobiose / cellulose), concentration and temperature. For each sample there will thus be one free parameter, the rotational activation energy  $E_R$ , and this will have to correctly model both the  $T_1$  and  $T_2$  full temperature dependences simultaneously.

In Figure 3 the dashed lines are the resultant fits of equation (2) to the pure ionic liquid and glucose samples. Fits to all the carbohydrates were equally good as the selection for glucose shown in Figure 3. The global fitting parameters found are  $\tau_0$  equal to  $2.4 \pm 0.1 \times 10^{-15}$  s and  $K$  equal to  $1.7 \pm 0.1 \times 10^9$  s<sup>-2</sup>. The value of  $\tau_0$  will be discussed later on. From equation (2c) the parameter  $K$  gives a very reasonable value for the effective distance between protons  $r$  of  $2.16 \pm 0.02 \times 10^{-10}$  m. Comparatively, a rough estimation gives the distance, or lattice spacing, between protons of  $2.64 \times 10^{-10}$  m (taking the molecular weight of [C2mim][OAc] at 170 g/mol, the density of the ionic liquid as 1.1 g/cm<sup>3</sup>,<sup>33</sup> the number of protons per molecule 14 and assuming that the protons are on a cubic lattice). This is remarkably close to the value determined through the NMR relaxometry

analysis, especially given such a simple calculation, and thus supports the quantitative validity of the BPP analysis applied here.

In our recent article<sup>37</sup> we argued that the ions in these carbohydrate systems behaved as an “ideal mixture” of free and associated ions. It was shown theoretically that for this ideal mixture rule to correctly describe the diffusion of the ions, the activation energy for their translational diffusion needed to be linear with respect to the associated fraction  $\alpha$ . This was verified experimentally for diffusion of [C2mim][OAc] in glucose / cellobiose / cellulose solutions. In Figure 6 we likewise plot the rotational activation energy as determined from the BPP analysis of the low field relaxometry data. The activation energy results all follow a linear dependence as a function of associated fraction of ions, suggesting that the rotational motion also obeys an ideal mixture rule. Since both rotational and translational motions are governed by  $\alpha$ , then the effective local microscopic viscosity experienced by the ions must also be determined by this parameter. In other words, the number of carbohydrate OH groups within these solutions dictates the dynamics of the ions.

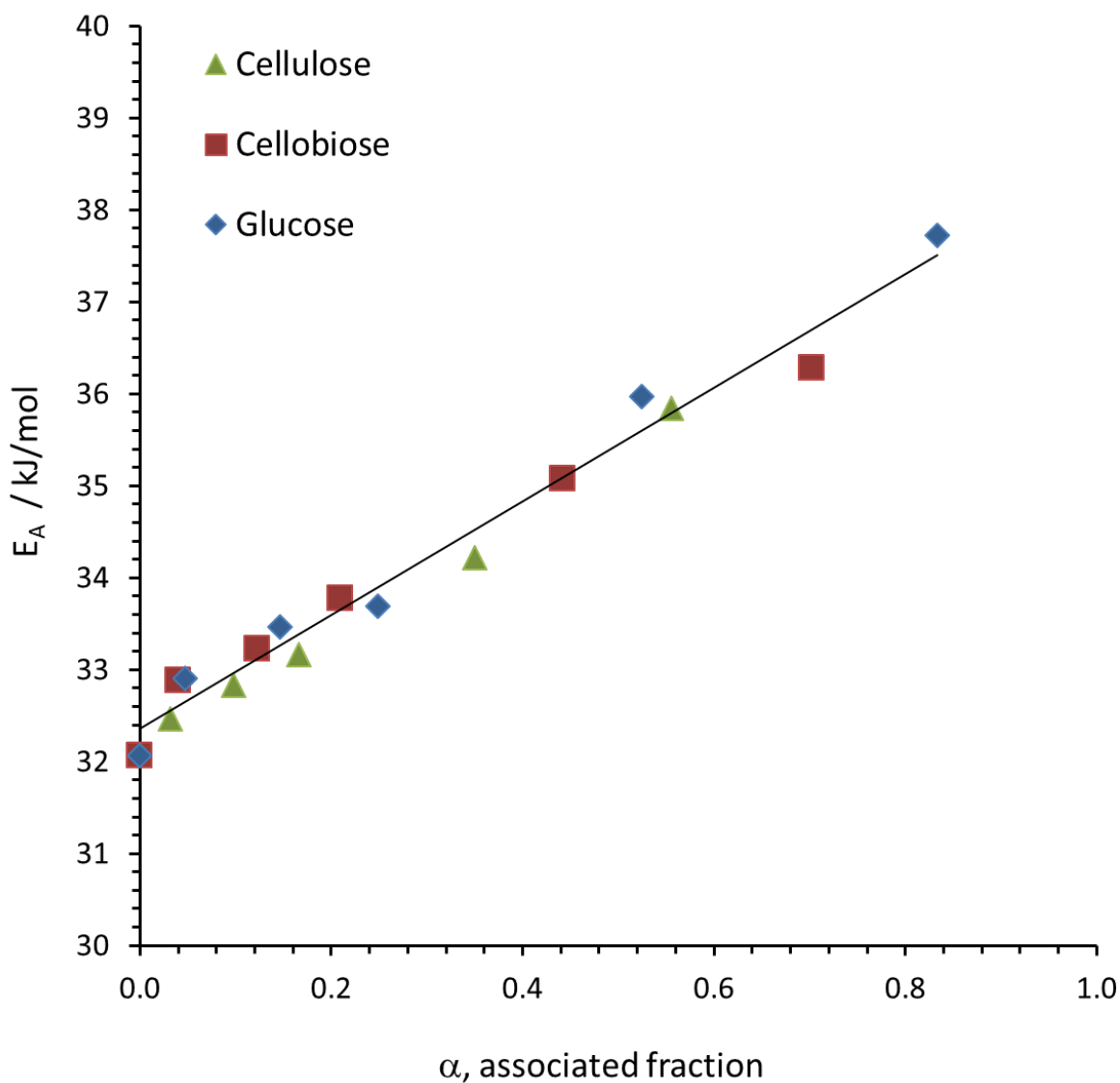


**Figure 6.** Activation energies of the correlation time  $\tau$ , found from BPP analysis using equations (2) and (3), plotted against associated fraction. The straight line is a fit to all the data presented, with an  $R^2$  of 0.98. Error bars are within the size of the symbols shown. The global fitting parameter is  $\tau_0 = 2.4 \pm 0.1 \times 10^{-15}$  s, which gives  $\tau_R$  values  $\sim 0.1$  ns across the temperature range studied here.

The extra “cost” in terms of additional activation energy for rotation of an ion due to its association with an OH group from a carbohydrate molecule is given directly by the gradient of the solid line in Figure 6 as  $6.2 \pm 0.5$  kJ/mol, which is reasonably close to the values found previously<sup>37</sup> for the increase in diffusional activation energy for being associated with an OH group of a carbohydrate molecule of  $8.2 \pm 0.4$  kJ/mol and  $7.6 \pm 0.4$  kJ/mol for the anion and cation respectively. Therefore, there is across the full range of associated fractions  $\alpha$  an approximately constant difference between the rotational activation energy and the corresponding diffusional activation energy of  $14 \pm 2$  kJ/mol,<sup>37</sup> with the diffusional motion having the higher energy barrier.

In the seminal work by Powell, Roseveare, and Eyring, a theory of viscosity, diffusion, thermal, and ionic conductivities in terms of a statistical mechanical theory for reaction rate was developed.<sup>52</sup> For flow to take place a single molecule moves past its neighbor and falls into a vacant equilibrium position, termed a hole or vacancy. An activation energy is required for a molecule to jump over its neighbor. The authors showed that there was a close link between viscous flow and vaporization, because the same bonds that need to be broken for flow to take place are required to be broken for vaporization.<sup>52</sup> In mixtures the ease of molecular flow is not determined predominantly by its own properties, but by the “solvent” or surrounding molecules that must contribute holes for it to flow into. In 1968, O’Reilly investigated the diffusion coefficients and rotational correlation times of several polar liquids.<sup>53</sup> In his work he argued that the difference between the activation energy for rotational motion and that for diffusional motion was due to the additional cost of creating the vacancy (or hole) for the diffusing molecule to move into. For both rotational and diffusional motion to occur all the close neighboring bonds must be broken, but for the diffusional translation there is the extra cost of creating the hole. This can be written mathematically as,<sup>53</sup>

$$D = D_0 \exp\left(-\frac{E_R + E_{hole}}{RT}\right) \quad (4)$$

where  $E_{hole}$  is the additional activation energy needed to create a vacancy into which the diffusing molecule can move into and, as argued above, has a value of  $14 \pm 2$  kJ/mol.

If we now continue to assume that the fluctuation correlation times  $\tau_R$  found from the BPP analysis are due to the rotational motion of the ions, it is then possible to theoretically predict the value for  $E_{hole}$  through the Stokes-Debye-Einstein relationship,<sup>51, 54</sup>

$$\tau_R = \frac{4\pi R_H^3 \eta}{3kT} \quad (5)$$

where  $R_H$  is the effective hydrodynamic radius of the molecule and  $k$  the Boltzmann constant.

The ratio of the viscosity to the temperature in equation (5) can be eliminated in favour of the diffusion coefficient through the Stokes-Einstein formula,<sup>51, 54</sup>

$$D = \frac{kT}{6\pi R_H \eta} \quad (6)$$

This gives,

$$\tau = \frac{2R_H^2}{9D} \quad (7)$$

Then combining this result with equations (3) and (4) obtains,

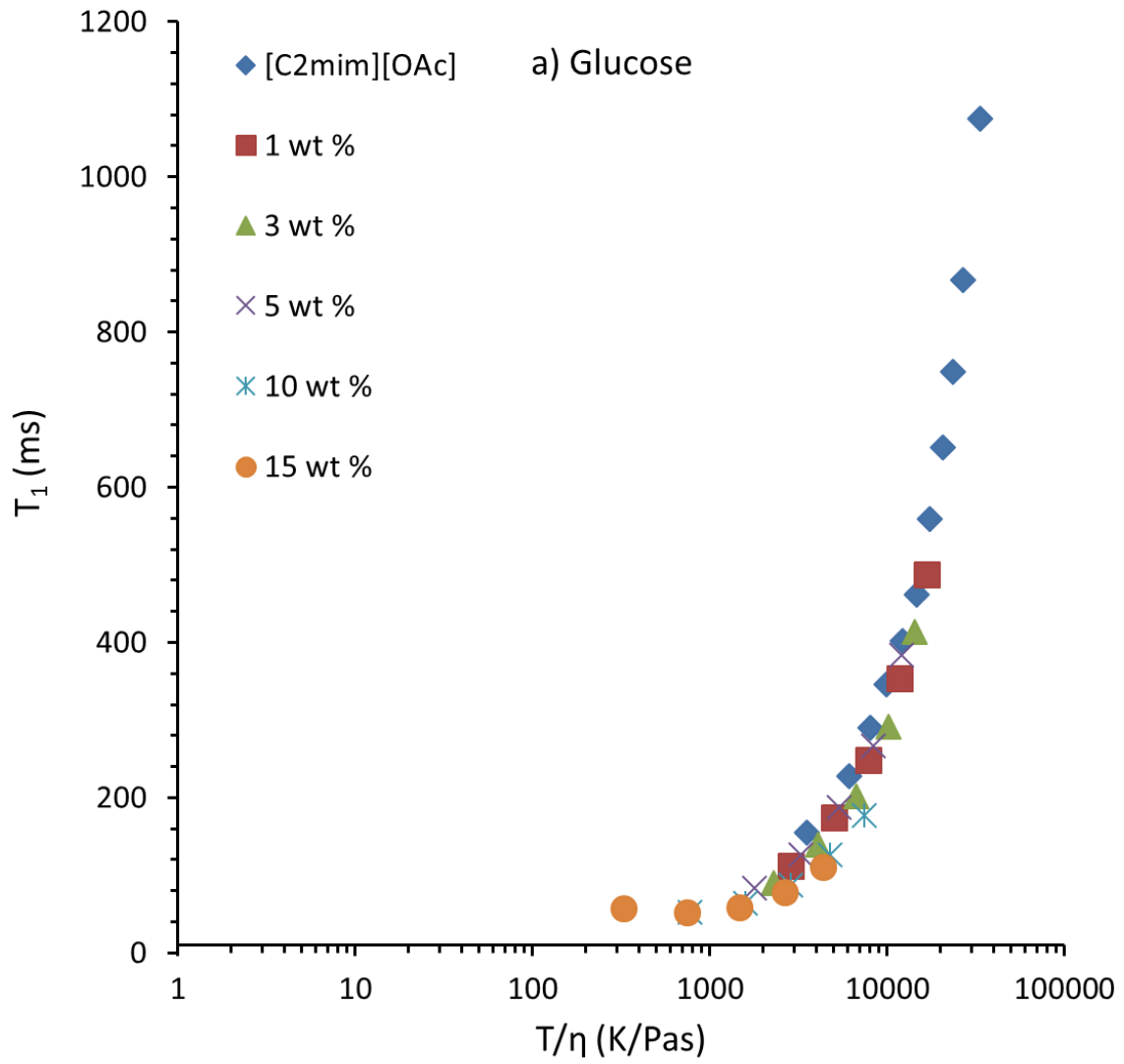
$$E_{hole} = RT \ln\left(\frac{9 D_0 \tau_0}{2 R_H^2}\right) \quad (8)$$

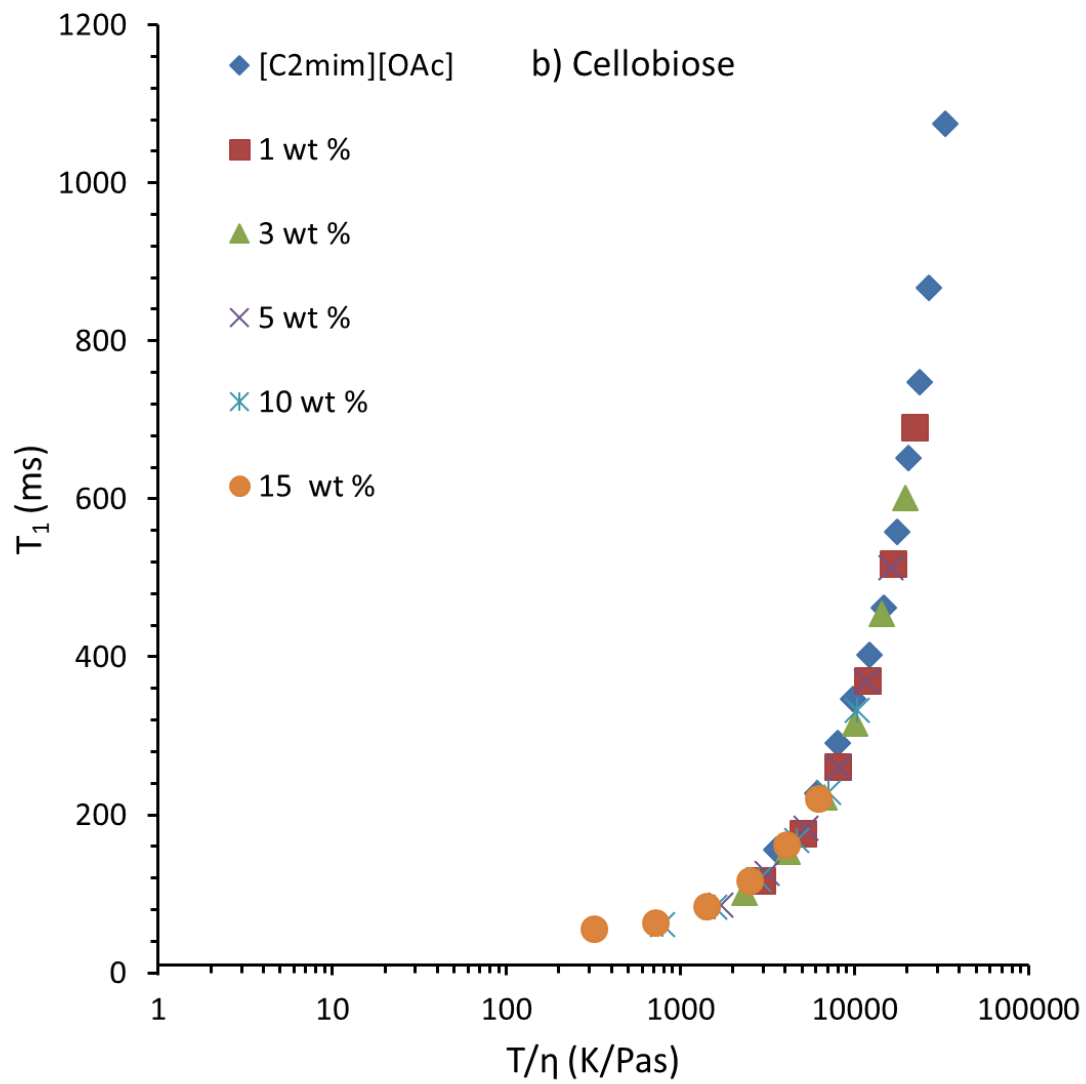
In the BPP analysis we obtain only one correlation time  $\tau_R$  and this is an effective average rotational time scale for the cations and anions in our system. To use equation (8) to estimate  $E_{hole}$  we take: i) the average value of  $D_0$  of  $1.5 \times 10^{-3} \text{ m}^2\text{s}^{-1}$  for the cation and anion ( $1.4 \pm 0.2 \times 10^{-3} \text{ m}^2\text{s}^{-1}$  and  $1.6 \pm 0.2 \times 10^{-3} \text{ m}^2\text{s}^{-1}$ , respectively<sup>37</sup>; and ii) the average value of hydrodynamic radii  $R_H$ ,  $2.5 \times 10^{-10} \text{ m}$ , of the cation and anion ( $2.8 \times 10^{-10} \text{ m}$  and  $2.2 \times 10^{-10} \text{ m}$ , respectively<sup>37</sup>) and  $\tau_0 = 2.4 \pm 0.1 \times 10^{-15}$

s from the above BPP analysis. Since our measurements span from 30 °C to 70 °C, we set  $T$  in equation (8) to an average value of 320 K (50 °C); all the temperatures in this study are within 6% of this middle value. Finally, combining all these parameters into equation (8) gives a prediction for  $E_{hole}$  of 15 kJ/mol, which is remarkably close to the measured value of  $14 \pm 2$  kJ/mol. This is strong support for taking the correlations time found from the relaxometry measurements through the BPP analysis as rotational correlation times; it also indicates that the parameters found from this approach are quantitatively correct.

When  $\tau_R$  and  $D$  are compared, as in the above analysis, then one microscopic term is being compared with another microscopic term. The quantitative agreement found above indicates that there is one effective microscopic viscosity that determines both the rotational and translational motion of the ions. This local microscopic viscosity can be altered by either varying the temperature and/or changing the number of solute OH groups for the ions to interact with, and it makes no difference whether those OH groups come from glucose, or cellobiose or indeed cellulose molecules. But what is interesting now is to compare the microscopic environment with the macroscopic one. This can be done by plotting  $T_l$ , which as we have shown is determined by microscopic rotational motion, against  $T/\eta$ , as is done in Figure 7.







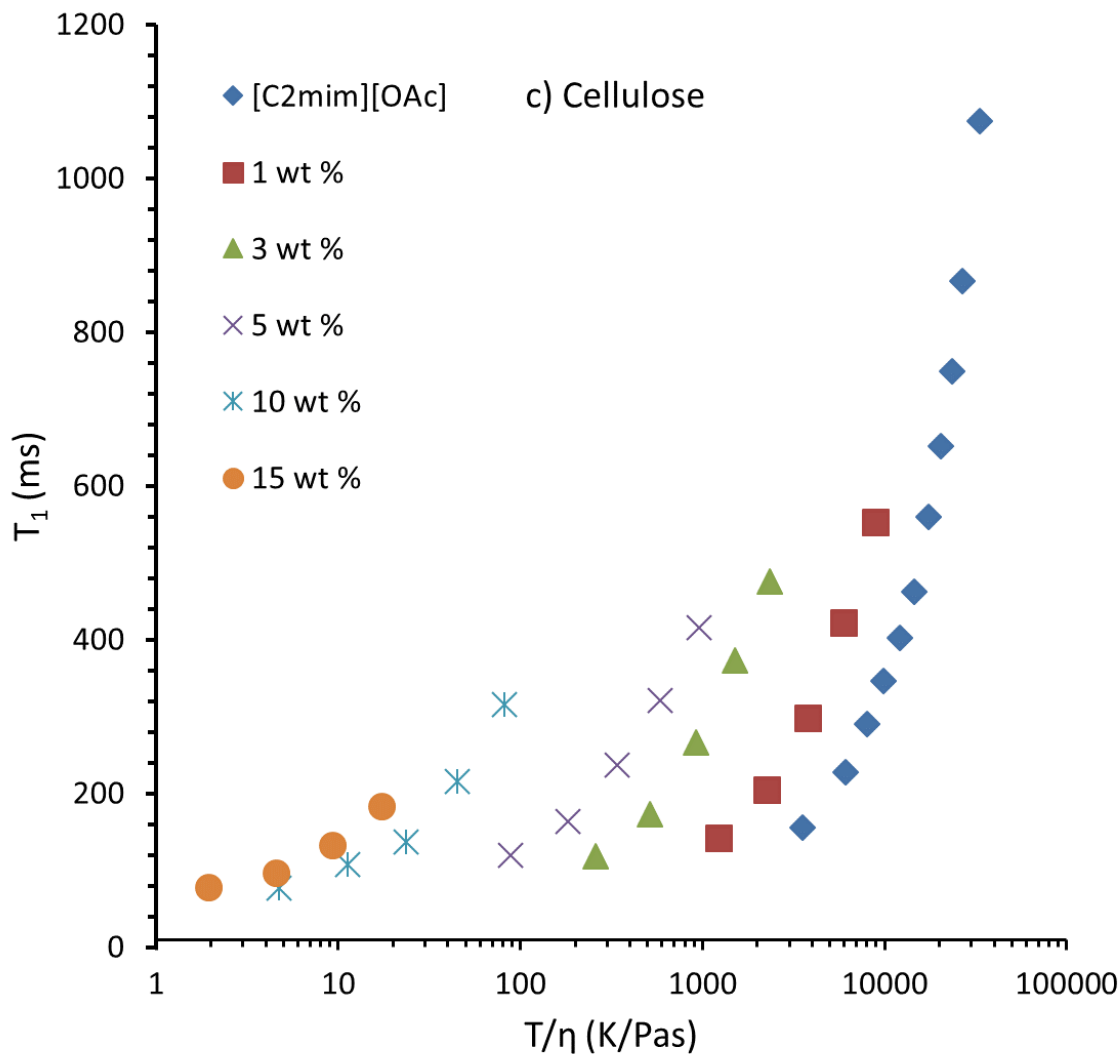


**Figure 7.** Spin-lattice relaxation time  $T_1$  against temperature over viscosity for a) glucose, b) cellobiose and c) cellulose samples at various carbohydrate concentrations in wt %. Error bars are within the size of the symbols shown.

The zero shear rate viscosity  $\eta$  is a macroscopic term, measured using a rheometer, and thus here large scale effects relative to the size of ions, such as polymer entanglements, play a

significant role in determining the resultant macroscopic viscosity. However, they play an almost insignificant role in determining the microscopic viscosity that determines the rotational and translational motions of the ions: for glucose and cellobiose all data at various concentrations fall on one master plot (Figures 7 a and b, respectively), which is not the case for cellulose (Figure 7c). For the glucose and cellobiose solutions the macroscopic and microscopic viscosities are proportional to each other, both being affected in a similar manner by changes in temperature and solute concentration. This is not the case for the cellulose solutions, with macroscopic viscosity dramatically increasing when macromolecules<sup>55</sup> are added into a solvent, especially above the overlap concentration (here, around<sup>56</sup> 1 wt%), as expected. On the length scale of the ions the local microviscosity within the cellulose samples is similar to that of the glucose and cellobiose samples; the key determining factor on these local length scales is the density of OH groups that the ions interact with.

#### **4. CONCLUSIONS**

In this work we analysed carbohydrate solutions in ionic liquid [C2mim][OAc] by measuring: i) the relaxation times of protons of ionic liquid probed by NMR relaxometry at 20 MHz and ii) viscosity of these solutions. The carbohydrates were glucose, cellobiose and cellulose, and each set of solutions was of five concentrations (1, 3, 5, 10, and 15 wt %). Each solution was measured at temperatures from 30 and 70 °C. Cellulose is found to be the most effective in increasing the solution viscosity as compared to glucose and cellobiose. In contrast, glucose was found to be the most effective in reducing the NMR relaxation times and cellulose the least effective. As the NMR relaxation times can be related to the mobility of the ions, this indicates that the ions in the most viscous set of samples have, counterintuitively, the highest mobility. A similar surprising result

was found when these samples were investigated previously<sup>37</sup> using pulsed field gradient NMR to determine the self-diffusion coefficients of the ions.

We demonstrated that it is the number of carbohydrate OH groups per repeating “glucose” unit that determines the mobility of the ions. We introduced<sup>37</sup> the parameter  $\alpha$ , which quantifies the molar ratio of OH groups per ionic liquid molecule. As glucose has more OH groups per repeat unit, then for any corresponding weight concentrations these samples will have a higher number of OH groups for the ions to interact with. It is these interactions that slow down the rotational and translational motion of the ions and, as a consequence, this loss of mobility reduces the NMR relaxation times. When the NMR relaxation times are plotted not as a function of weight concentration, but instead against  $\alpha$ , then all data fall on master curves independent of particular carbohydrate. This is strong evidence that the molar density of OH groups is the most important factor in determining the microscopic environment of the ions.

The NMR relaxation times were analyzed in terms of the theoretical<sup>40</sup> work of Bloembergen, Purcell and Pound. For each sample at each temperature a correlation time  $\tau_R$  was found. The activation energies for this correlation time were shown to be linearly dependent on  $\alpha$  and this reveals that these solutions can be considered as ideal mixtures of associated and non-associated ions.

For an associated ion there is the additional cost for rotation,  $6.2 \pm 0.5$  kJ/mol, compared to that for a free ion. From previous work on the diffusion of ions in these same systems,<sup>37</sup> translational motion involves a higher activation energy, an extra  $14 \pm 2$  kJ/mol, than that for rotational motion obtained in this work. We interpreted this additional barrier stemming from the need of a hole or vacancy to form in translational motion.<sup>52</sup> By using Stokes-Debye-Einstein equations linking viscosity to rotation and diffusion, combined with the fitting parameters from the NMR

relaxometry analysis, it was possible to predict this additional cost quite accurately (15 kJ/mol). This supports our interpretation that the correlation times  $\tau_R$  found are predominantly arising from rotational motion. The success of equation (8) is quite remarkable, in that it uses two parameters  $D_0$  and  $\tau_0$  that are not usually the subjects of Arrhenius-type analysis, which when coupled with the average hydrodynamic radius of the ions calculates the activation energy in forming a vacancy for translational motion. This then predicts the difference between how diffusion and rotation change as a function of temperature. This is strong evidence for the quantitative nature of our analysis and supports our interpretation that the NMR relaxometry can be related to the rotational motion of the ions.

Finally, this work highlights important differences between what is occurring microscopically and macroscopically in a carbohydrate ionic liquid mixture. Macroscopically, the viscosity depends on the volume occupied by the solute. Microscopically, the dominant factor is the number of OH groups on a carbohydrate molecule, the effect of which can be quantified by the associated fraction  $\alpha$ .

## **ACKNOWLEDGEMENT**

S.M.G. is funded by an EPSRC CASE Award (EP/I501495/1) with Innovia Films (Wigton, Cumbria, CA7 9BG, UK). M.E.R. is a Royal Society Industry Fellow (IF120090). The data for this article can be found at doi: <https://doi.org/10.5518/369>

## REFERENCES

1. Walden, P., Molecular magnitude and electrical conductivity of some fused salts. *Bulletin de l'Academie Imperiale des Sciences de St. Petersburg* **1914**, (6), 405-422.
2. Angell, C. A.; Ansari, Y.; Zhao, Z. F., Ionic Liquids: Past, present and future. *Faraday Discuss.* **2012**, *154*, 9-27.
3. Plechkova, N. V.; Seddon, K. R., Applications of ionic liquids in the chemical industry. *Chemical Society Reviews* **2008**, *37* (1), 123-150.
4. Short, P. L., Out of the Ivory tower. *Chemical & Engineering News* **2006**, *84* (17), 15-+.
5. Wang, H.; Gurau, G.; Rogers, R. D., Ionic liquid processing of cellulose. *Chem. Soc. Rev.* **2012**, *41* (4), 1519-1537.
6. Welton, T., Room-temperature ionic liquids. Solvents for synthesis and catalysis. *Chemical Reviews* **1999**, *99* (8), 2071-2083.
7. Zhu, S.; Chen, R.; Wu, Y.; Chen, Q.; Zhang, X.; Yu, Z., A Mini-Review on Greenness of Ionic Liquids. *Chem. Biochem. Eng. Q.* **2009**, *23* (2), 207-211.
8. Zhu, S. D.; Wu, Y. X.; Chen, Q. M.; Yu, Z. N.; Wang, C. W.; Jin, S. W.; Ding, Y. G.; Wu, G., Dissolution of cellulose with ionic liquids and its application: a mini-review. *Green Chemistry* **2006**, *8* (4), 325-327.
9. Graenacher, C. Cellulose solution. US Pat. 1943176, 1934.
10. Swatloski, R. P.; Spear, S. K.; Holbrey, J. D.; Rogers, R. D., Dissolution of cellose with ionic liquids. *J. Am. Chem. Soc.* **2002**, *124* (18), 4974-4975.
11. Klemm, D.; Heublein, B.; Fink, H. P.; Bohn, A., Cellulose: Fascinating biopolymer and sustainable raw material. *Angewandte Chemie-International Edition* **2005**, *44* (22), 3358-3393.
12. Medronho, B.; Romano, A.; Miguel, M. G.; Stigsson, L.; Lindman, B., Rationalizing cellulose (in)solubility: reviewing basic physicochemical aspects and role of hydrophobic interactions. *Cellulose* **2012**, *19* (3), 581-587.
13. Sescousse, R.; Le, K. A.; Ries, M. E.; Budtova, T., Viscosity of Cellulose-Imidazolium-Based Ionic Liquid Solutions. *Journal Of Physical Chemistry B* **2010**, *114* (21), 7222-7228.
14. French, A. D., Glucose, not cellobiose, is the repeating unit of cellulose and why that is important. *Cellulose* **2017**, *24* (11), 4605-4609.
15. Glasser, W. G.; Atalla, R. H.; Blackwell, J.; Brown, R. M.; Burchard, W.; French, A. D.; Klemm, D. O.; Nishiyama, Y., About the structure of cellulose: debating the Lindman hypothesis. *Cellulose* **2012**, *19* (3), 589-598.
16. Bharadwaj, V. S.; Schutt, T. C.; Ashurst, T. C.; Maupin, C. M., Elucidating the conformational energetics of glucose and cellobiose in ionic liquids. *Phys. Chem. Chem. Phys.* **2015**, *17* (16), 10668-10678.
17. Gentile, L.; Olsson, U., Cellulose-solvent interactions from self-diffusion NMR. *Cellulose* **2016**, *23* (4), 2753-2758.
18. Green, S. M.; Ries, M. E.; Moffat, J.; Budtova, T., NMR and Rheological Study of Anion Size Influence on the Properties of Two Imidazoliumbased Ionic Liquids. *Scientific Reports* **2017**, *7*.
19. Han, N.; Wang, X. F.; Qu, T. S.; Qian, Y. Q.; Lu, Y. H., Preparation and Properties of Cellulose Benzoate and Preliminary Exploration About Cellulose Benzoate-g-polyoxyethylene(2) Hexadecyl Ether. *Chemical Journal of Chinese Universities-Chinese* **2017**, *38* (6), 1099-1106.

20. Hedlund, A.; Kohnke, T.; Theliander, H., Diffusion in Ionic Liquid-Cellulose Solutions during Coagulation in Water: Mass Transport and Coagulation Rate Measurements. *Macromolecules* **2017**, *50* (21), 8707-8719.
21. Hegde, G. A.; Bharadwaj, V. S.; Kinsinger, C. L.; Schutt, T. C.; Pisierra, N. R.; Maupin, C. M., Impact of water dilution and cation tail length on ionic liquid characteristics: Interplay between polar and non-polar interactions. *Journal of Chemical Physics* **2016**, *145* (6).
22. Isik, M.; Sardon, H.; Mecerreyes, D., Ionic Liquids and Cellulose: Dissolution, Chemical Modification and Preparation of New Cellulosic Materials. *International Journal of Molecular Sciences* **2014**, *15* (7), 11922-11940.
23. Jia, L. Y.; Pedersen, C. M.; Qiao, Y.; Deng, T. S.; Zuo, P. P.; Ge, W. Z.; Qin, Z. F.; Hou, X. L.; Wang, Y. X., Glucosamine condensation catalyzed by 1-ethyl-3-methylimidazolium acetate: mechanistic insight from NMR spectroscopy. *Phys. Chem. Chem. Phys.* **2015**, *17* (35), 23173-23182.
24. Kimura, M.; Shinohara, Y.; Takizawa, J.; Ren, S.; Sagisaka, K.; Lin, Y. D.; Hattori, Y.; Hinestroza, J. P., Versatile Molding Process for Tough Cellulose Hydrogel Materials. *Scientific Reports* **2015**, *5*.
25. Norman, S. E.; Turner, A. H.; Holbrey, J. D.; Youngs, T. G. A., Solvation Structure of Uracil in Ionic Liquids. *Chemphyschem* **2016**, *17* (23), 3923-3931.
26. Radhi, A.; Le, K. A.; Ries, M. E.; Budtova, T., Macroscopic and Microscopic Study of 1-Ethyl-3-methyl-imidazolium Acetate-DMSO Mixtures. *Journal of Physical Chemistry B* **2015**, *119* (4), 1633-1640.
27. Schuermann, J.; Huber, T.; LeCorre, D.; Mortha, G.; Sellier, M.; Duchemin, B.; Staiger, M. P., Surface tension of concentrated cellulose solutions in 1-ethyl-3-methylimidazolium acetate. *Cellulose* **2016**, *23* (2), 1043-1050.
28. Schutt, T. C.; Bharadwaj, V. S.; Hegde, G. A.; Johns, A. J.; Maupin, C. M., In silico insights into the solvation characteristics of the ionic liquid 1-methyltriethoxy-3-ethylimidazolium acetate for cellulosic biomass. *Phys. Chem. Chem. Phys.* **2016**, *18* (34), 23715-23726.
29. Singh, V.; Panda, S.; Kaur, H.; Banipal, P. K.; Gardas, R. L.; Banipal, T. S., Solvation behavior of monosaccharides in aqueous protic ionic liquid solutions: Volumetric, calorimetric and NMR spectroscopic studies. *Fluid Phase Equilibria* **2016**, *421*, 24-32.
30. Zhang, C.; Liu, R. G.; Xiang, J. F.; Kang, H. L.; Liu, Z. J.; Huang, Y., Dissolution Mechanism of Cellulose in N,N-Dimethylacetamide/Lithium Chloride: Revisiting through Molecular Interactions. *Journal of Physical Chemistry B* **2014**, *118* (31), 9507-9514.
31. Zhang, J. M.; Wu, J.; Yu, J.; Zhang, X. Y.; He, J. S.; Zhang, J., Application of ionic liquids for dissolving cellulose and fabricating cellulose-based materials: state of the art and future trends. *Materials Chemistry Frontiers* **2017**, *1* (7), 1273-1290.
32. Zhang, J. M.; Xu, L. L.; Yu, J.; Wu, J.; Zhang, X. Y.; He, J. S.; Zhang, J., Understanding cellulose dissolution: effect of the cation and anion structure of ionic liquids on the solubility of cellulose. *Science China-Chemistry* **2016**, *59* (11), 1421-1429.
33. Hall, C. A.; Le, K. A.; Rudaz, C.; Radhi, A.; Lovell, C. S.; Damion, R. A.; Budtova, T.; Ries, M. E., Macroscopic and Microscopic Study of 1-Ethyl-3-methyl-imidazolium Acetate-Water Mixtures. *J. Phys. Chem. B* **2012**, *116* (42), 12810-12818.
34. Lovell, C. S.; Walker, A.; Damion, R. A.; Radhi, A.; Tanner, S. F.; Budtova, T.; Ries, M. E., Influence of Cellulose on Ion Diffusivity in 1-Ethyl-3-Methyl-Imidazolium Acetate Cellulose Solutions. *Biomacromolecules* **2010**, *11* (11), 2927-2935.



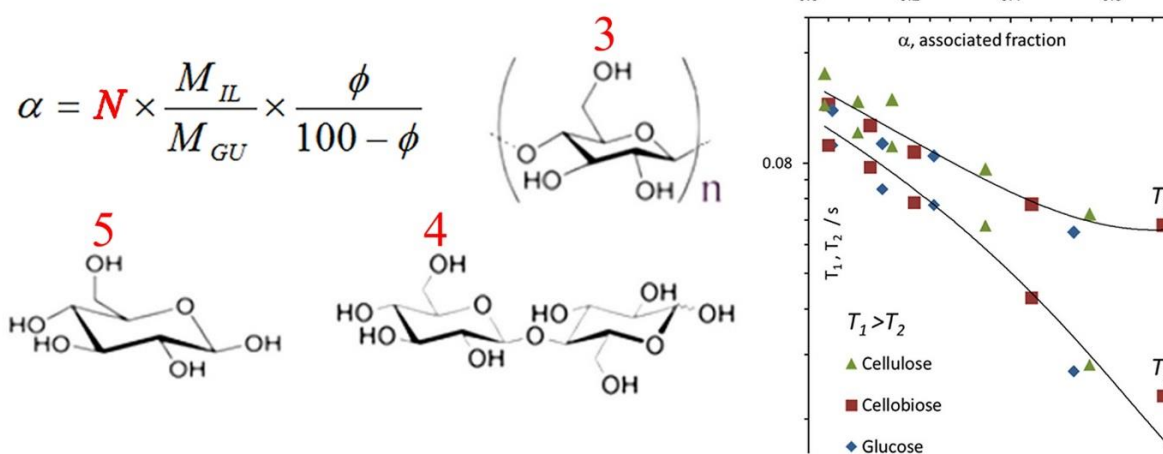
35. Ries, M. E.; Budtova, T.; Radhi, A., NMR relaxometry, diffusion, and rheology studies of carbohydrates in ionic liquids. *Abstracts of Papers of the American Chemical Society* **2014**, 247, 1.
36. Ries, M. E.; Budtova, T.; Radhi, A.; Ovenden, J.; Keating, A.; Parker, O., NMR studies of carbohydrate solvation in the room temperature ionic liquid 1-ethyl-3-methyl-imidazolium acetate. *Abstracts of Papers of the American Chemical Society* **2013**, 245, 1.
37. Ries, M. E.; Radhi, A.; Keating, A. S.; Parker, O.; Budtova, T., Diffusion of 1-Ethyl-3-methyl-imidazolium Acetate in Glucose, Cellobiose, and Cellulose Solutions. *Biomacromolecules* **2014**, 15 (2), 609-617.
38. D'Agostino, C.; Mantle, M. D.; Mullan, C. L.; Hardacre, C.; Gladden, L. F., Diffusion, Ion Pairing and Aggregation in 1-Ethyl-3-Methylimidazolium-Based Ionic Liquids Studied by H-1 and F-19 PFG NMR: Effect of Temperature, Anion and Glucose Dissolution. *Chemphyschem* **2018**, 19 (9), 1081-1088.
39. Zhao, Y. L.; Liu, X. M.; Wang, J. J.; Zhang, S. J., Insight into the Cosolvent Effect of Cellulose Dissolution in Imidazolium-Based Ionic Liquid Systems. *Journal of Physical Chemistry B* **2013**, 117 (30), 9042-9049.
40. Bloembergen, N.; Purcell, E. M.; Pound, R. V., Relaxation Effects In Nuclear Magnetic Resonance Absorption. *Physical Review* **1948**, 73 (7), 679-712.
41. Clough, M. T.; Geyer, K.; Hunt, P. A.; Son, S.; Vagt, U.; Welton, T., Ionic liquids: not always innocent solvents for cellulose. *Green Chemistry* **2015**, 17 (1), 231-243.
42. Carr, H. Y.; Purcell, E. M., Effects of Diffusion on Free Precession in Nuclear Magnetic Resonance Experiments. *Physical Review* **1954**, 94 (3), 630-638.
43. Angell, C. A., Formation of glasses from liquids and biopolymers. *Science* **1995**, 267 (5206), 1924-35.
44. Callaghan, P. T., *Principles of Nuclear Magnetic Resonance Microscopy*. Clarendon Press: Oxford, 1992; p 492.
45. Daniel, C. I.; Chavez, F. V.; Feio, G.; Portugal, C. A. M.; Crespo, J. G.; Sebastiao, P. J., H-1 NMR Relaxometry, Viscometry, and PFG NMR Studies of Magnetic and Nonmagnetic Ionic Liquids. *Journal of Physical Chemistry B* **2013**, 117 (39), 11877-11884.
46. Daniel, C. I.; Chavez, F. V.; Portugal, C. A. M.; Crespo, J. G.; Sebastiao, P. J., H-1 NMR Relaxation Study of a Magnetic Ionic Liquid as a Potential Contrast Agent. *Journal of Physical Chemistry B* **2015**, 119 (35), 11740-11747.
47. Driver, G. W.; Huang, Y.; Laaksonen, A.; Sparrman, T.; Wang, Y. L.; Westlund, P. O., Correlated/non-correlated ion dynamics of charge-neutral ion couples: the origin of ionicity in ionic liquids. *Phys. Chem. Chem. Phys.* **2017**, 19 (7), 4975-4988.
48. Neves, L. A.; Sebastiao, P. J.; Coelho, I. M.; Crespo, J. G., Proton NMR Relaxometry Study of Nafion Membranes Modified with Ionic Liquid Cations. *Journal of Physical Chemistry B* **2011**, 115 (27), 8713-8723.
49. Seyedlar, A. O.; Stapf, S.; Mattea, C., Dynamics of the ionic liquid 1-butyl-3-methyl-imidazolium bis(trifluoromethylsulphonyl)imide studied by nuclear magnetic resonance dispersion and diffusion. *Phys. Chem. Chem. Phys.* **2015**, 17 (3), 1653-1659.
50. Blicharska, B.; Peemoeller, H.; Witek, M., Hydration water dynamics in biopolymers from NMR relaxation in the rotating frame. *Journal of Magnetic Resonance* **2010**, 207 (2), 287-293.
51. Carper, W. R.; Mains, G. J.; Piersma, B. J.; Mansfield, S. L.; Larive, C. K., C-13 NMR relaxation and H-1 diffusion (DOSY) studies of an acidic chloroaluminate melt. *Journal Of Physical Chemistry* **1996**, 100 (12), 4724-4728.

52. Powell, R. E.; Roseveare, W. E.; Eyring, H., Diffusion, thermal conductivity, and viscous flow of liquids. *Industrial and Engineering Chemistry* **1941**, *33*, 430-435.
53. O'Reilly, D. E., SELF-DIFFUSION COEFFICIENTS AND ROTATIONAL CORRELATION TIMES IN POLAR LIQUIDS. *Journal of Chemical Physics* **1968**, *49* (12), 5416-5420.
54. Antony, J. H.; Dolle, A.; Mertens, D.; Wasserscheid, P.; Carper, W. R.; Wahlbeck, P. G., C-13 NMR relaxation rates in the ionic liquid 1-methyl-3-nonylimidazolium hexafluorophosphate. *Journal Of Physical Chemistry A* **2005**, *109* (30), 6676-6682.
55. Staudinger, H.; Heuer, W., Highly polymerized compounds. XCIV. An insoluble polystyrene. *Ber.* **1934**, *67B*, 1164-72.
56. Gericke, M.; Schlufte, K.; Liebert, T.; Heinze, T.; Budtova, T., Rheological Properties of Cellulose/Ionic Liquid Solutions: From Dilute to Concentrated States. *Biomacromolecules* **2009**, *10* (5), 1188-1194.

# For Table of Contents Use Only

Microscopic and macroscopic properties of carbohydrate solutions in the ionic liquid 1-ethyl-3-methyl-imidazolium acetate

Michael E. Ries, Asanah Radhi, Stephen M Green, Jamie Moffat and Tatiana Budtova



**Keywords:** cellulose, cellobiose, glucose, carbohydrate, ionic liquid, NMR, relaxometry, viscosity, diffusion.

# Supporting Information

## Microscopic and macroscopic properties of carbohydrate solutions in the ionic liquid 1-ethyl-3- methyl-imidazolium acetate

Michael E. Ries <sup>a,\*</sup>, Asanah Radhi <sup>a</sup>, Stephen M Green <sup>a</sup>, Jamie Moffat <sup>b</sup> and Tatiana Budtova <sup>c</sup>

<sup>a</sup> Soft Matter Physics Research Group, School of Physics and Astronomy, University of Leeds,  
Leeds, LS2 9JT. UK.

<sup>b</sup> Innovia Films R&D Centre, West Road, Wigton, Cumbria CA7 9XX, United Kingdom

<sup>c</sup> MINES ParisTech, PSL Research University, Center for Materials Forming (CEMEF), UMR  
CNRS 7635, CS 10207, 06904 Sophia Antipolis, France.

[m.e.ries@leeds.ac.uk](mailto:m.e.ries@leeds.ac.uk)

Data for this publication can be found at doi: <https://doi.org/10.5518/369>

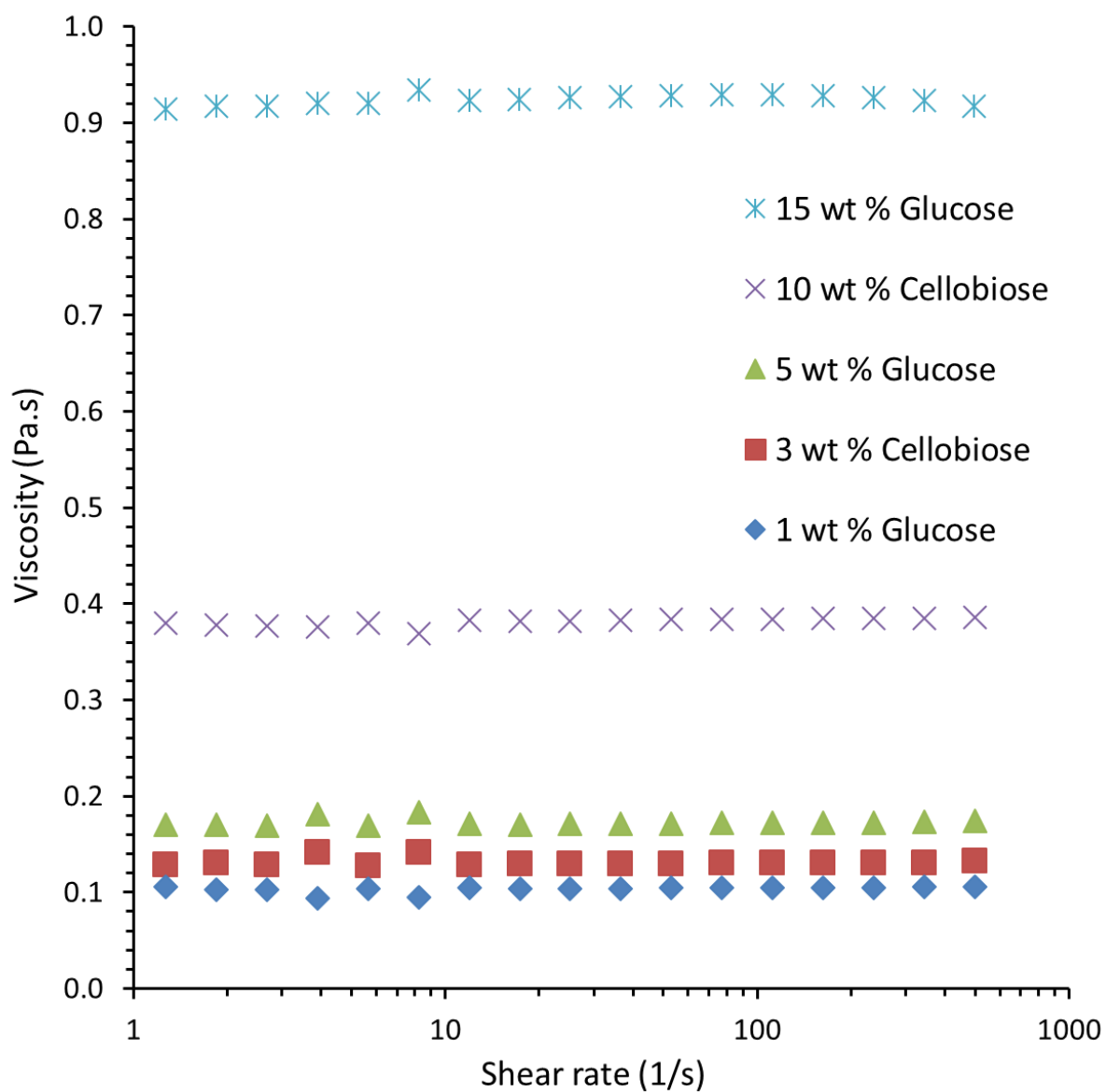


**Figure S11.** Viscosity against shear rate of carbohydrate-[C2mim][OAc] solutions at different concentrations of carbohydrates at 30 °C. Error bars are within the size of the symbols shown.

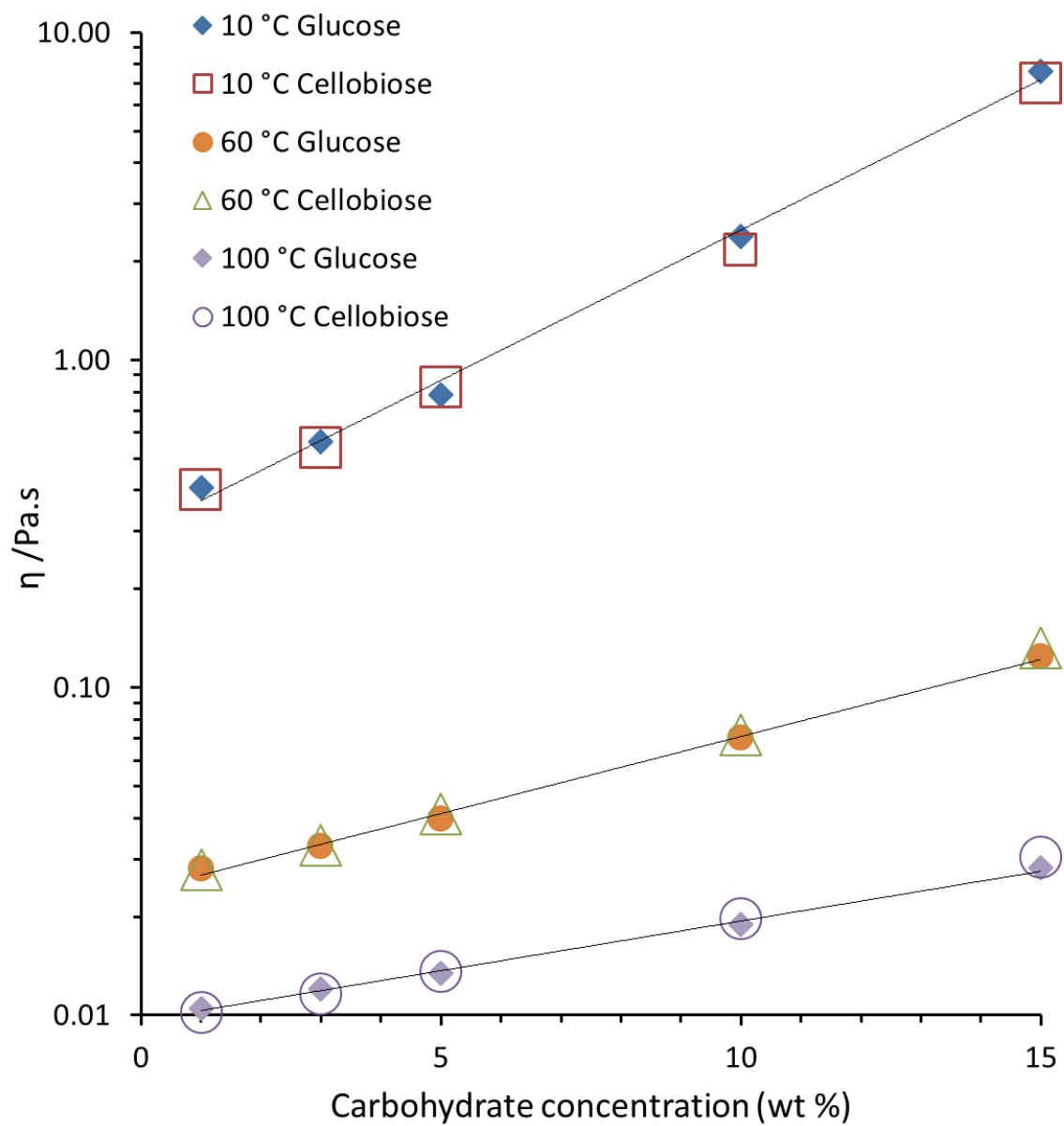


**Figure SI2.** Viscosity at 10 °C, 60 °C and 100 °C for the glucose and cellobiose in [C2mim][OAc] solutions, against carbohydrate concentration. The straight lines are guides to the eye. Error bars are within the size of the symbols shown.

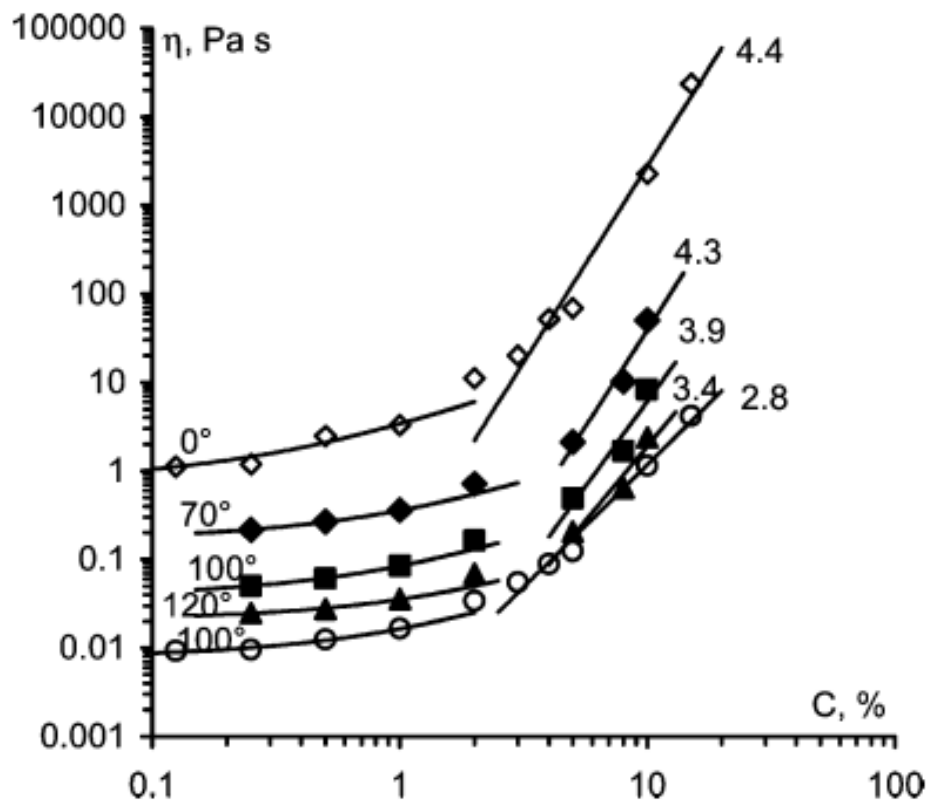


**Figure 3.** Viscosity–concentration dependence for cellulose–BMIMCl (dark symbols) and cellulose–EMIMAc (open symbols) solutions at various temperatures shown directly at the corresponding data. Lines are linear (in the dilute region) and power-law (in the semidilute region) approximations. Power-law exponents are shown for each set of data. The errors are of the size of symbols.

**Figure SI3.** Viscosity of cellulose [C2mim][OAc] solutions against cellulose concentration.

Reprinted with permission from {Journal of Physical Chemistry B, volume 114 page 7224-7228, 2010}. Copyright {2010} American Chemical Society.

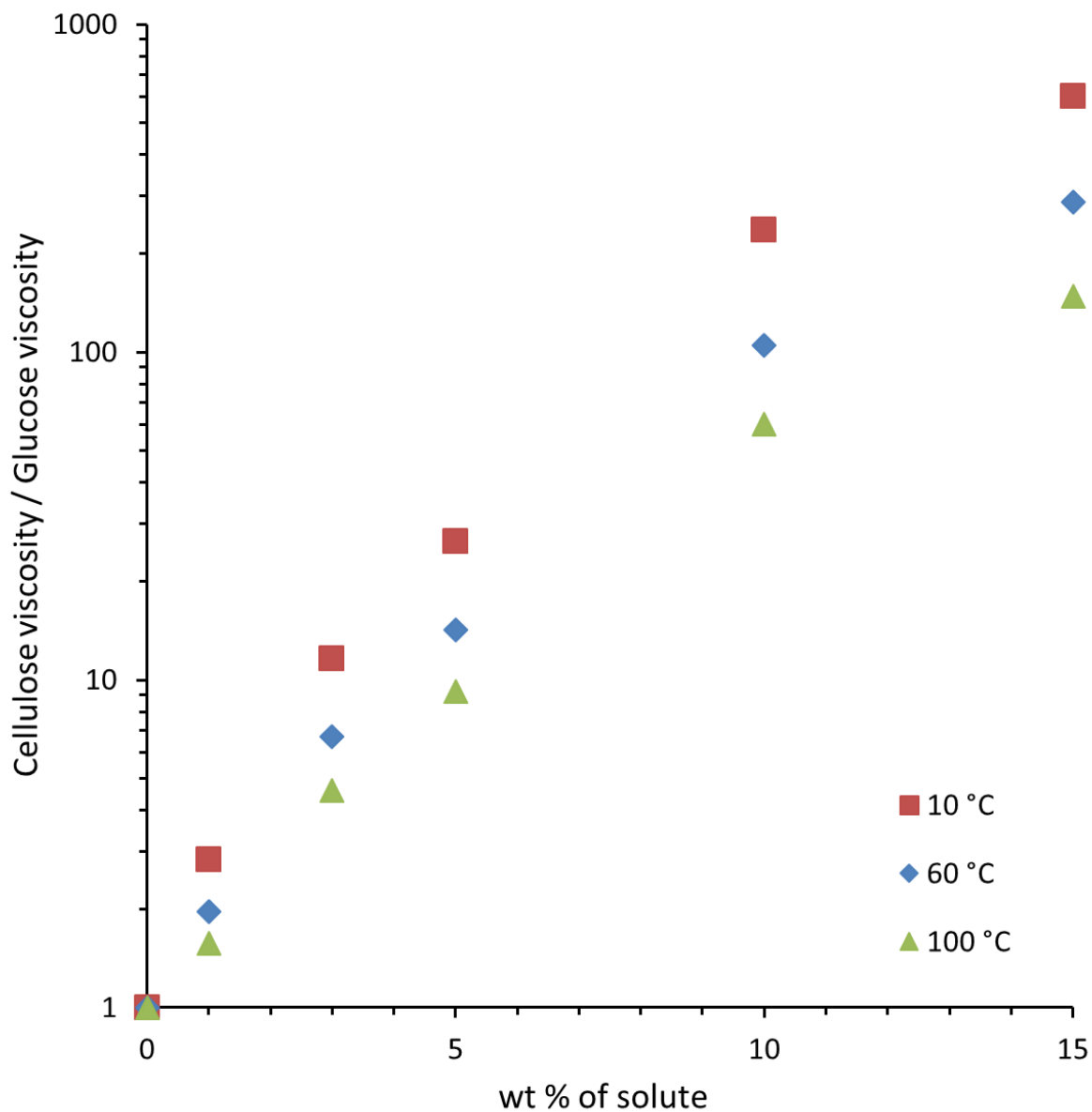


**Figure SI4.** Viscosity ratio of cellulose to glucose in [C2mim][OAc] solutions (at the same solute concentrations), against solute carbohydrate concentration.



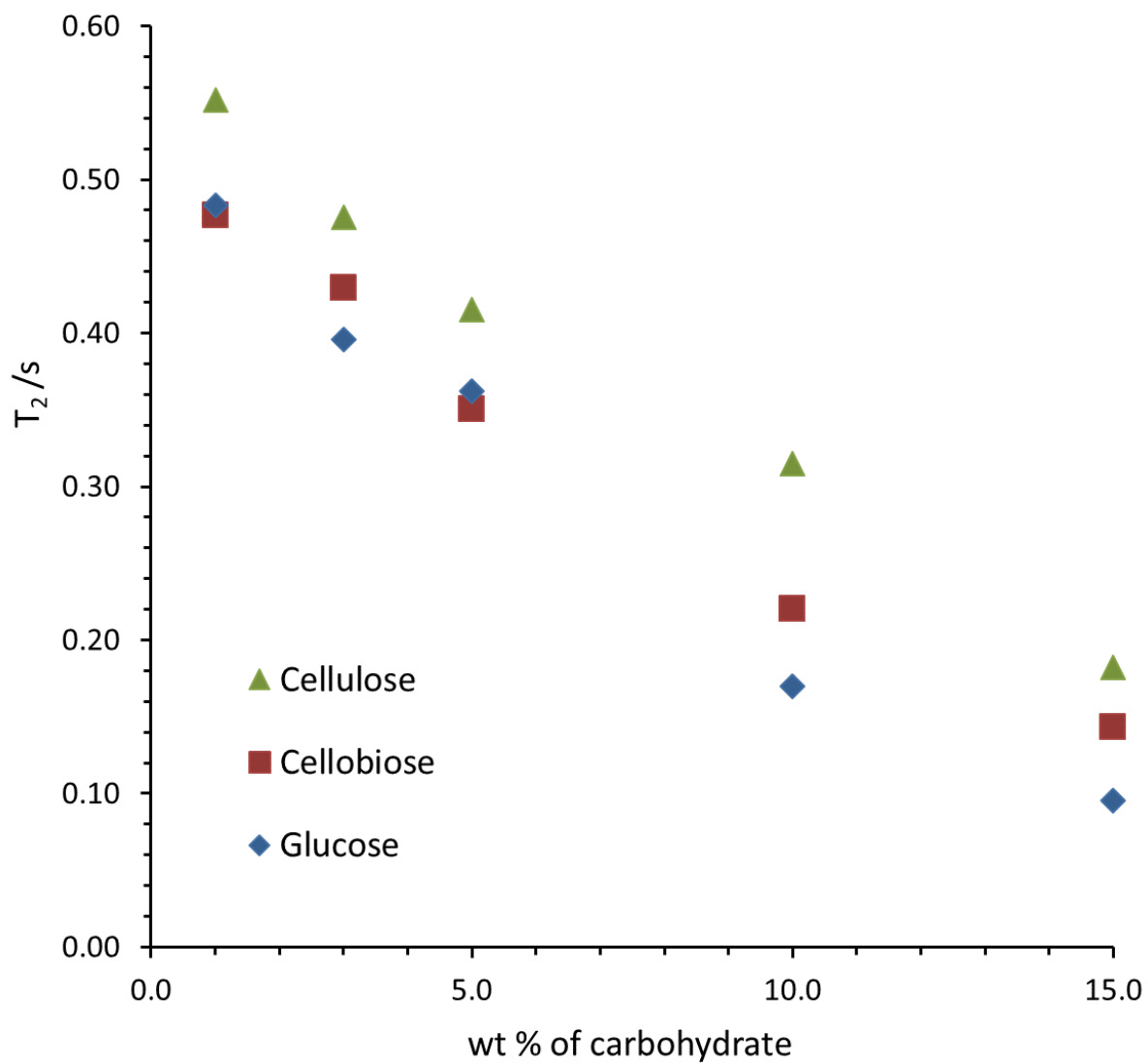


**Figure SI5.** NMR spin-lattice relaxation times  $T_2$  for glucose, cellobiose and cellulose as a function of the wt % of carbohydrate in [C2mim][OAc] solutions at 70 °C. Uncertainties are within the size of the symbols used.